SEPTEMBER 1976 MATT-1258

TWO-DIMENSIONAL SPATIAL STRUCTURE OF THE DISSIPATIVE TRAPPED-ELECTRON MODE

BY

G. REWOLDT, W. M. TANG,
AND E. A. FRIEMAN

PLASMA PHYSICS LABORATORY

PRINCETON UNIVERSITY
PRINCETON, NEW JERSEY

This work was supported by U. S. Energy Research and Development Administration Contract E(11-1)-3073. Reproduction, translation, publication, use and disposal, in whole or in part, by or for the United States Government is permitted.

DISCLAIMER

NOTICE

Printed in the United States of America.

Available from
National Technical Information Service
U. S. Department of Commerce
5285 Port Royal Road
Springfield, Virginia 22151

Price: Printed Copy $ * ; Microfiche $1.45

*Pages	NTIS Selling Price
1-50	$ 4.00
51-150	5.45
151-325	7.60
326-500	10.60
501-1000	13.60

Two-Dimensional Spatial Structure of the Dissipative Trapped-Electron Mode

G. Rewoldt, W. M. Tang and E. A. Frieman
Plasma Physics Laboratory, Princeton University
Princeton, New Jersey 08540

ABSTRACT

This paper deals with the complete two-dimensional structure of the dissipative trapped-electron mode over its full width, which may extend over several mode-rational surfaces. The complete integro-differential equation is studied in the limit $k_r\rho_i < 1$, where ρ_i is the ion gyroradius, and k_r, the radial wavenumber, is regarded as a differential operator. This is converted into a matrix equation which is then solved by standard numerical methods. Solutions obtained are in reasonably good agreement with one-dimensional analytic solutions, in the limits where such results are expected to be valid. More significantly, the present approach can readily treat many physically important cases for which purely analytic solutions are difficult to obtain. The results indicate that the differential equation formulation of the eigenmode equation is valid only for long wavelength modes ($k_\theta\rho_i \lesssim 0.3$, with k_θ being the poloidal wavenumber). For such cases it is found that shear stabilization estimates obtained from the one-dimensional radial solution are quite inaccurate for modes overlapping only a small number of mode-rational surfaces, but become more accurate for modes overlapping many mode-rational surfaces.

-OT E(11-1)-3073

I. INTRODUCTION

The dissipative trapped-electron mode is expected to have important consequences in tokamaks, and accordingly, has been the subject of many previous studies. However, previous investigations of the linear stage of the mode have generally been one-dimensional. In particular, either the radial structure of the mode is ignored while solving for the structure parallel to a magnetic field line,[1,2] or the parallel structure is ignored while solving for the radial structure in the vicinity of a single mode-rational surface.[3] This paper deals with the complete two-dimensional structure of the mode over its full width, which may extend over several mode-rational surfaces. The complete integro-differential equation is studied in the limit $k_r \rho_i < 1$, (where k_r, the radial wavenumber, is regarded as a differential operator and ρ_i is the ion gyroradius) for the case of a circular cross-section, large aspect ratio tokamak with concentric magnetic surfaces. The perturbed electrostatic potential is expanded in complete sets of radial and poloidal basis functions, thereby converting it into a matrix equation, for which eigenvalues and eigenvectors may be obtained by standard numerical methods. These eigenfunctions for the perturbed electrostatic potential satisfy all periodicity requirements in the presence of magnetic shear. Also, the effects of temperature gradients and of magnetic curvature and gradient drifts are included for both electrons and ions. Electron collisions are accounted for by means of the simplest energy-dependent Krook collision operator,

while ion collisons are neglected. Mode-particle resonance terms for circulating ions and electrons are included, while those for trapped particles are omitted. Magnetic drift effects within these resonance terms are omitted; this is equivalent to neglect of finite radial excursion (banana width) effects. The reasons for these approximations and omissions are given in the following sections.

Comparison of the numerical solutions obtained with one-dimensional analytic solutions indicate reasonable agreement in the limits where the analytic results are expected to be valid. However, it should be emphasized here that the present analysis is applicable to many physically relevant cases which cannot be treated by previous methods. In particular, the stabilizing effect of magnetic shear can be compared with estimates obtained from the radial one-dimensional analysis mentioned above, (i.e., from the solution of Weber's equation). For modes overlapping only a few mode-rational surfaces, the one-dimensional estimates for growth rates are quite inaccurate. The net effect of the additional mode-rational surfaces is stabilizing for the case considered, indicating that energy absorption there dominates energy reflection. For modes overlapping many mode-rational surfaces, the radial one-dimensional results and the two-dimensional results are surprisingly close, indicating that the net effect of all of the additional mode-rational surfaces is small. The final conclusion about shear stabilization from the two-dimensional results is the same as that obtained from the radial

one-dimensional results, namely, that for normal gradients and realistic tokamak parameters, the amount of shear is not sufficient to stabilize the mode, while with the additional strong stabilizing effect of oppositely directed density and temperature gradients,[4] the amount of shear can be sufficient for stabilization. However, it should be emphasized that the actual spatial structure of the unstable modes is found to be very different from the structure calculated using the one-dimensional radial analysis. An upper limit on k_θ, the poloidal wavenumber, for the validity of the differential formulation for finite ion-Larmor radius effects is obtained. It is found to be quite low, $k_\theta \rho_i \lesssim 0.3$, and in fact, excludes a very important part of parameter space. Specifically, the local theory predicts the fastest growing instabilities to fall in the range $k_\theta \rho_i > 0.3$.

In Sec. II, the notation and the assumptions made about the equilibrium are explained, the form used for the perturbed electrostatic potential is discussed, and the results for the perturbed electron and ion densities are given. In Sec. III, the quasi-neutrality integro-differential equation is presented and the solution method discussed. In Sec. IV, numerical results are given and discussed, and in Sec. V conclusions are given. In Appendix A, the derivation for the perturbed electron density is given, and in Appendix B the derivation for the perturbed ion density is given. In Appendix C, forms for magnetic drift frequencies are obtained, and computationally convenient forms for terms entering the integro-differential equation are derived.

II. PERTURBED ELECTRON AND ION DENSITIES

A. Notation and Equilibrium

In the coordinate system employed, ζ denotes the toroidal angle, θ the poloidal angle, r the minor radius of a magnetic surface, R_o the major radius of the magnetic axis, with $\theta = 0$ at the outside of the torus. The inverse aspect ratio is $\epsilon_o \equiv r/R_o \ll 1$. The form for the magnetic field corresponding to the assumption of concentric, circular cross-section magnetic surfaces is

$$\underset{\sim}{B} = [B_o \underset{\sim}{e}_\zeta + B_\theta^o(r)\underset{\sim}{e}_\theta]/h(\theta) \ , \tag{1}$$

where $h(\theta) \equiv 1 + \epsilon_o \cos\theta$. Along a magnetic field line

$$\frac{d\ell_{||}}{B} = \frac{Rd\zeta}{B_\zeta} = \frac{rd\theta}{B_\theta} \ , \tag{2}$$

where $\ell_{||}$ indicates length along a field line and $R = R_o h(\theta)$, so that the "safety factor" can be expressed as

$$q(r) \equiv \frac{rB_o}{R_o B_\theta^o} \simeq \left.\frac{d\zeta}{d\theta}\right|_{\text{field line}} \ . \tag{3}$$

Since $B_\theta^o \ll B_o$, q is of order unity and $B \equiv |\underset{\sim}{B}| \simeq B_o/h(\theta)$. In velocity space two different coordinate systems will be used, namely $v_{||}$ and $v_\perp$, indicating velocity components parallel and perpendicular to the equilibrium magnetic field, as well as the quantities $\varepsilon \equiv (m_j/2)(v_{||}^2 + v_\perp^2)$, the kinetic energy, and $\Lambda \equiv \mu B_o/\varepsilon$, the dimensionless pitch angle variable, where $\mu = (m_j/2)v_\perp^2/B$ is the magnetic moment, m_j is the particle mass,

and $j = e, i$ denote electrons and ions respectively. The ions have charge $e_i = +|e|$ and the electrons charge $e_e = -|e|$. The parallel velocity has the form

$$v_{||} = \sigma_{||} \left[\frac{2}{m_j}(\varepsilon - \mu B)\right]^{1/2} = \sigma_{||} v [1 - \Lambda/h(\theta)]^{1/2} , \qquad (4)$$

where $\sigma_{||} = \text{sign}(v_{||})$. Circulating particles correspond to $0 \leq \Lambda < 1 - \varepsilon_o$ and trapped particles to $1 - \varepsilon_o < \Lambda \leq 1 + \varepsilon_o$. The trapped particle turning points are $\pm \theta_o = \pm \arccos [(\Lambda - 1)/\varepsilon_o]$.

The equilibrium electric field $\underset{\sim}{E}^{(o)}$ is assumed equal to zero. Then the single particle constants of the motion are ε, Λ, and the toroidal canonical angular momentum

$$P_\zeta \simeq m_j R (v_\zeta - \Omega_{\theta j} r) \simeq m_j R_o (v_{||} - \Omega^o_{\theta j} r) , \qquad (5)$$

where $\Omega_{\theta j} \equiv e_j B_\theta / m_j c$ and $\Omega^o_{\theta j} \equiv e_j B^o_\theta / m_j c$.

The bounce period τ_b for trapped particles is given by

$$\tau_b = \oint dt = \oint \frac{d\theta}{v_{||}} \frac{rB}{B_\theta} = qR_o \oint \frac{d\theta}{v_{||}(\theta)} \equiv 2qR_o \int_{-\theta_o}^{\theta_o} d\theta / |v_{||}(\theta)| . \qquad (6)$$

Likewise, the transit period for a circulating particle is

$$\tau_t = qR_o \int_{-\pi}^{\pi} d\theta / v_{||}(\theta) . \qquad (7)$$

The corresponding bounce and transit frequencies are defined as $\omega_b \equiv 2\pi/\tau_b$ and $\omega_t \equiv 2\pi/\tau_t$ respectively. Note that $\tau_b, \omega_b > 0$, while $\text{sign}(\tau_t, \omega_t) = \text{sign}(v_{||}) = \sigma_{||}$, by convention, and that τ_b is equivalent to $2|\tau_t|$ at the boundary between trapped and circulating particles.

The equilibrium distribution function is taken to be $f_j^{(o)} = f_{mj}(1 + \hat{f}_j)$, where $\hat{f}_j \ll 1$,

$$f_{mj} \equiv \frac{n(r)}{[2\pi T_j(r)/m_j]^{3/2}} \exp\left[-\varepsilon/T_j(r)\right] , \tag{8}$$

and

$$\hat{f}_j \equiv -\frac{v_\zeta}{\Omega_{\theta j}}\left[\frac{1}{n}\frac{dn}{dr} - \frac{1}{T_j}\frac{dT_j}{dr}\left(\frac{3}{2} - \frac{\varepsilon}{T_j}\right)\right] , \tag{9}$$

where T_j is the temperature in energy units. "Neoclassical" corrections for the circulating particles are neglected. These corrections were shown in Ref. 5 to have only a small effect on the results.

In terms of the variables ε and Λ , the integral over velocity space becomes

$$\int d^3\underset{\sim}{v} = \frac{\pi}{2}\left(\frac{2}{m_j}\right)^{3/2} \sum_{\sigma_{||}} \int_0^\infty d\varepsilon\ \varepsilon^{1/2} \int_0^{h(\theta)} d\Lambda \frac{1}{h(\theta)\left[1-\Lambda/h(\theta)\right]^{1/2}} . \tag{10}$$

at a fixed value of θ . The notation

$$\langle \ldots \rangle_j \equiv \frac{1}{n}\int d^3\underset{\sim}{v}\, f_{Mj} \ldots , \tag{11}$$

will be used. The integration will sometimes be over only the trapped (or circulating) particles, as will be clear from the context. Note that

$$\langle |\omega_t| \rangle_j \simeq \bar{\omega}_{tj} \equiv \frac{v_j}{qR_o} , \tag{12}$$

and

$$\langle \omega_b \rangle_j \simeq \left(\frac{\epsilon_0}{2}\right)^{1/2} \bar{\omega}_{tj} , \tag{13}$$

where $v_j \equiv (2T_j/m_j)^{1/2}$.

B. Mode Properties

Considering $\beta = 8\pi n(T_e + T_i)/B_o^2 \ll 1$, the electrostatic approximation can be made for the perturbed electric field

$$\underset{\sim}{E}^{(1)} = -\nabla\tilde{\Phi} . \tag{14}$$

By virtue of axisymmetry, for the linear stage of the mode the perturbed electrostatic potential $\tilde{\Phi}$ can be written as

$$\tilde{\Phi}(r,\theta,\zeta,t) = \tilde{\phi}_\ell(\theta,r)\exp(-i\omega t + i\ell\zeta), \tag{15}$$

where ℓ , the toroidal mode number, is an integer. It is convenient to choose a "reference" mode-rational surface at $r = r_o$ in the radial region of interest, around which the mode is to be localized, such that $q(r_o) = m^o/\ell$. The "slow" and "fast" θ-dependence can then be separated without loss of generality, i.e.,

$$\tilde{\Phi}(r,\theta,\zeta,t) = \tilde{\phi}(\theta,r)\exp(-i\omega t + i\ell\zeta - im^o\theta), \tag{16}$$

where m^o , the poloidal mode number, is an integer, and $\tilde{\phi}(\theta,r)$ must be periodic in θ with period 2π , and $|[(\partial/\partial\theta)\tilde{\phi}]/\tilde{\phi}| \ll m^o$.

The radial distance from r_o in units of the spacing of mode-rational surfaces is now defined by the new radial variable

$$S(r) \equiv \ell q(r) - m^o = \ell[q(r) - q(r_o)] , \tag{17}$$

with $S(r_o) = 0$. Note that $S(r) \simeq (r - r_o)/\Delta r_s$, where $\Delta r_s \equiv [\ell(dq/dr)]^{-1} \equiv [\ell q']^{-1}$ is the spacing of mode-rational surfaces, and d^2q/dr^2 is neglected. In terms of $S(r)$,

$$\tilde{\Phi} = [\tilde{\phi}(\theta,S) \exp(iS\theta)] \exp\{i\ell[\zeta - q(r)\theta]\} \exp(-i\omega t) \quad . \tag{18}$$

Since $[\zeta - q(r)\theta]$ is approximately constant along a field line, the variation of $\tilde{\Phi}$ along the field line is given by $\tilde{\phi}(\theta,S) \exp(iS\theta)$. In particular

$$\frac{\partial}{\partial \ell_{||}} \tilde{\Phi} = \frac{1}{qR_o} \exp\{i\ell[\zeta - q(r)\theta] - i\omega t\} \frac{\partial}{\partial \theta}[\tilde{\phi}(\theta,S) \exp iS\theta]$$

$$= \frac{1}{qR_o} \exp\{i\ell[\zeta - q(r)\theta] - i\omega t\} \exp(iS\theta) \left(\frac{\partial}{\partial \theta} + iS\right) \tilde{\phi}(\theta,S) \quad , \tag{19}$$

to lowest order in ϵ_o .

C. Perturbed Electron Density

The form of the perturbed electron density response is derived in Appendix A. It is valid in the limits $|\Omega_e| \gg \langle\omega_b\rangle_e \gg \omega$ and $k_\perp \rho_e \ll 1$, which are the usual parameter ranges of interest in dealing with low-frequency drift modes. Here $\Omega_e \equiv -|e|B_o/m_e c$, $\rho_e \equiv v_e/|\Omega_e|$, and $k_\perp$ is the wavenumber perpendicular to the magnetic field. To obtain the perturbed electron distribution function, the linearized drift kinetic equation is solved by means of an expansion in bounce and transit frequency harmonics, and an integration along unperturbed particle orbits. For simplicity, an energy-dependent Krook model, with the effective electron collision frequency given by $\nu_f(\varepsilon) = (\nu_e/\varepsilon_o)(T_e/\varepsilon)^{3/2}$, has been employed to account for the

dominant effects of collisions. As demonstrated in work using the actual Fokker-Planck operator[6] and a number-conserving form of the BGK operator,[7] this simple Krook operator provides reasonably accurate results in the electrostatic limit.

The perturbed electron density is $n_e^{(1)} \equiv \tilde{n}_e \exp(-i\omega t + i\ell\zeta - im^o\theta)$, where

$$\tilde{n}_e \equiv \frac{|e|n}{T_e}\left[\phi(\theta,S) - \left(\frac{2}{\pi^{1/2}h(\theta)}\right.\right.$$

$$\times\int_0^\infty dX\, X^2 \exp(-X^2)\,\{\omega - \omega_{*e}[1+\eta_e(X^2-3/2)]\}$$

$$\times\int_{1-\epsilon_o}^{h(\theta)} d\Lambda[1-\Lambda/h(\theta)]^{-1/2}\ \frac{\Phi^{(o)}(\Lambda,\theta,S)}{\omega + i(\nu_e/\epsilon_o)X^{-3} - \omega_{De}^{(o)}X^2}$$

$$+\ i\frac{\pi^{1/2}}{h(\theta)}\sum_{\sigma_{||}}\int_0^{1-\epsilon_o} d\Lambda\,[1-\Lambda/h(\theta)]^{-1/2}\sum_{p=-\infty}^{\infty}\sum_{j''=1}^{5}$$

$$\times\tilde{\Phi}^{(p)}(\Lambda,\theta,S)\exp[ip\omega_t\hat{t}(\theta)]\left|(p+S)\hat{\omega}_t + 2\omega_{De}^{(o)}X_{j''}\right.$$

$$\left.\left.+\,3i(\nu_e/\epsilon_o)X_{j''}^{-4}\right|^{-1}X_{j''}^2\exp(-X_{j''}^2)$$

$$\left.\times\{\omega - \omega_{*e}[1+\eta_\epsilon(X_{j''}^2-3/2)]\}\right)\Bigg]. \qquad (20)$$

Here $X \equiv (\varepsilon/T_e)^{1/2}$, $\omega_{*e} \equiv [\ell c T_e/(|e|R_o B_\theta^o)](d\ \ell n\, n/dr)$ $= [m^o c T_e/|e|r_o B_o)](d\ \ell n\, n/dr)$, and $\eta_e \equiv (d\ \ell n\, T_e/dr)/(d\ \ell n\, n/dr)$. Also ω_{De} is the electron magnetic drift frequency, whose detailed form is given in Appendices A and C. The superscript zero indicates a time average along a single particle orbit. A "hat" (^) indicates that the X-dependence has been factored out of a quantity. The quantity $\tilde{\Phi}^{(o)}$ is the time-averaged

perturbed potential seen by a trapped particle, while $\tilde{\phi}^{(p)}$ is the coefficient function for the p-th transit frequency harmonic of the perturbed potential for a circulating particle. Detailed forms of these quantities are given in Appendices A and C. The parametric time function $\hat{t}(\theta)$ along a circulating particle orbit is defined in Appendix A. The quantities X_j, represent the five roots of the polynomial

$$\omega + i(\nu_e/\epsilon_o)X^{-3} - \hat{\omega}_{De}^{(o)}X^2 - (p+S)\hat{\omega}_t X = 0 \ . \tag{21}$$

In Eq. (20) the three terms are the adiabatic term, the trapped-electron time-averaged term, and the circulating-electron resonance term.

D. Perturbed Ion Density

The derivation of the perturbed ion distribution function is quite similar to that for electrons, and is given in Appendix B. One important difference is that effects of finite $k_\perp \rho_i$ need to be included. Note that

$$i\underset{\sim}{k}_\perp \tilde{\Psi} \cong \nabla_\perp \tilde{\Phi} \simeq (\underset{\sim}{e}_r \frac{\partial}{\partial r} + \underset{\sim}{e}_\theta \frac{1}{r}\frac{\partial}{\partial \theta})\tilde{\phi}(\theta,S) \exp(-i\omega t + i\ell\zeta - im^o\theta)$$

$$\simeq \exp(-i\omega t + i\ell\zeta - im^o\theta)(\underset{\sim}{e}_r \frac{\partial}{\partial r} - \underset{\sim}{e}_\theta i\frac{m^o}{r})\tilde{\phi}(\theta,S) \ , \tag{22}$$

for $\epsilon_o \ll 1$, so that $k_r = -i(\partial/\partial r)$ and $k_\theta = (-m^o/r)$. Then the important finite ion gyroradius effects can be included by inserting a factor $J_o^2(k_\perp v_\perp/\Omega_i)$, where J_o is the Bessel function of the first kind, into the nonadiabatic term in the expression for

the perturbed ion distribution function.[5] The resultant expression is then expanded for $k_r\rho_i < 1$ with k_r replaced by $-i(\partial/\partial r)$.

The perturbed ion density is $n_i^{(1)} = \tilde{n}_i \exp(-i\omega t + i\ell\zeta - im^o\theta)$, with $\tilde{n}_i = \tilde{n}_i^{NR} + \tilde{n}_i^{R}$. The nonresonant part $\tilde{n}_i^{NR}$, before expansion for small $k_r\rho_i$, in terms of $b_i = b_{i\theta} + b_{ir}$ $\equiv (\rho_i^2/2)(k_\theta^2 + k_r^2)$, is

$$\begin{aligned}
\tilde{n}_i^{NR} = -\frac{|e|n}{T_i}\Bigg(1 - e^{-b_i}\Bigg\{&\left(1 - \frac{\omega_{*i}}{\omega}\right)I_o - \eta_i\,\frac{\omega_{*i}}{\omega}\,b_i(I_1 - I_o) \\
&- \left|\left(1 - \frac{\omega_{*i}}{\omega}\right)I_o - \eta_i\,\frac{\omega_{*i}}{\omega}[I_o + b_i(I_1 - I_o)]\right|\,\frac{\bar{\omega}_{ti}^2}{2\omega^2}\left(\frac{\partial}{\partial\theta} + iS\right)^2 \\
&+ \left(1 - \frac{\omega_{*i}}{\omega}\right)\left(\frac{\bar{\omega}_{Di}\cos\theta}{\omega}\right)[I_o(2 - b_i) + I_1 b_i] \\
&- \eta_i\,\frac{\omega_{*i}}{\omega}\left(\frac{\bar{\omega}_{Di}\cos\theta}{\omega}\right)[I_o(2 - 4b_i + 2b_i^2) + I_1(3b_i - 2b_i^2)] \\
&+ \left(1 - \frac{\omega_{*i}}{\omega}\right)\left(\frac{\bar{\omega}_{Di}\cos\theta}{\omega}\right)^2[I_o(7 - 6b_i + 2b_i^2) + I_1(5b_i - 2b_i^2)] \\
&- \eta_i\,\frac{\omega_{*i}}{\omega}\left(\frac{\bar{\omega}_{Di}\cos\theta}{\omega}\right)^2[I_o(14 - 25b_i + 19b_i^2 - 4b_i^3) \\
&+ I_1(17b_i - 17b_i^2 + 4b_i^3)] + \ldots\Bigg\}\Bigg)\tilde{\phi}(\theta,S) \ . \qquad (23)
\end{aligned}$$

Here $\omega_{*i} \equiv -(T_i/T_e)\omega_{*e}$, $\eta_i = (d\,\ell n\,T_i/dr)/(d\,\ell n\,n/dr)$, $\bar{\omega}_{Di}$ $\equiv \omega_{*i}(r_n/R_o)$, $r_n \equiv -(d\,\ell n\,n/dr)^{-1}$, $I_o = I_o(b_i)$ and $I_1 = I_1(b_i)$ are modified Bessel functions of the first kind, and $|\bar{\omega}_{Di}/\omega|$ and $|\bar{\omega}_{ti}/\omega|$ are taken to be small.

At this point b_i will be separated into $b_i = b_{i\theta} + b_{ir}$, with $b_{i\theta}$ arbitrary but with $b_{ir} < 1$. Specifically, the quantities b_{ir} , $(\bar{\omega}_{Di}/\omega)$, and $(\bar{\omega}_{ti}/\omega)$ will all be regarded

as small (of order α), and all terms through order α^2 will be kept. Expanding $\tilde{n}_i^{NR}$ to second order in a Taylor series in b_{ir} yields

$$\tilde{n}_i^{NR} = -\frac{|e|n}{T_i}\Bigg[1-\exp(b_{i\theta})\Bigg(\Big(1-\frac{\omega_{*i}}{\omega}\Big)\{I_o+b_{ir}(I_1-I_o)+(b_{ir}^2/2)$$

$$\times[2(I_o-I_1)-I_1/b_{i\theta}]\}-\eta_i\frac{\omega_{*i}}{\omega}\{b_{i\theta}(I_1-I_o)$$

$$-b_{ir}[I_o+2b_{i\theta}(I_1-I_o)]+(b_{ir}^2/2)[3I_o-I_1+4b_{i\theta}$$

$$\times(I_1-I_o)]\}-\Big[\Big(1-\frac{\omega_{*i}}{\omega}\Big)I_o-\eta_i\frac{\omega_{*i}}{\omega}[I_o+b_{i\theta}(I_1-I_o)]\Big]$$

$$\times\frac{\bar{\omega}_{ti}^2}{2\omega^2}\Big(\frac{\partial}{\partial\theta}+iS\Big)^2+\Big(1-\frac{\omega_{*i}}{\omega}\Big)\Big(\frac{\bar{\omega}_{Di}\cos\theta}{\omega}\Big)\{[I_o(2-b_{i\theta})+I_1b_{i\theta}]$$

$$+b_{ir}[I_o(2b_{i\theta}-3)+I_1(2-2b_{i\theta})]\}-\eta_i\frac{\omega_{*i}}{\omega}\Big(\frac{\bar{\omega}_{Di}\cos\theta}{\omega}\Big)$$

$$\times\{I_o(2-4b_{i\theta}+2b_{i\theta}^2)+I_1(3b_{i\theta}-2b_{i\theta}^2)$$

$$+b_{ir}[I_o(-6+11b_{i\theta}-4b_{i\theta}^2)$$

$$+I_1(2-9b_{i\theta}+4b_{i\theta}^2)]\}+\Big(1-\frac{\omega_{*i}}{\omega}\Big)$$

$$\times\Big(\frac{\bar{\omega}_{Di}\cos\theta}{\omega}\Big)^2[I_o(7-6b_{i\theta}+2b_{i\theta}^2)+I_1(5b_{i\theta}-2b_{i\theta}^2)]$$

$$-\eta_i\frac{\omega_{*i}}{\omega}\Big(\frac{\bar{\omega}_{Di}\cos\theta}{\omega}\Big)^2[I_o(14-25b_{i\theta}+19b_{i\theta}^2-4b_{i\theta}^3)+I_1$$

$$\times(17b_{i\theta}-17b_{i\theta}^2+4b_{i\theta}^3)]\Bigg)\Bigg]\tilde{\phi}(\theta,S), \qquad (24)$$

where now $I_o = I_o(b_{i\theta})$ and $I_1 = I_1(b_{i\theta})$.

The ion resonant term will be regarded as small (at least second order in α), so that only k_θ needs to be kept in the argument of the Bessel function J_o . Noting that $(k_\theta v_i/\Omega_i) = (2b_{i\theta}\Lambda)^{1/2}X$, to lowest order in ϵ_o , the resonant part of $\tilde{n}_i$ is

$$\tilde{n}_i^R = -\frac{|e|n}{T_i} i\frac{\pi^{1/2}}{h(\theta)}\sum_{\sigma_{||}}\int_o^{1-\epsilon_o} d\Lambda[1-\Lambda/h(\theta)]^{-1/2}\sum_{p=-\infty}^{\infty}\sum_{j"=1}^{2}$$

$$\times\tilde{\Phi}^{(p)}(\Lambda,\theta,S)e^{ip\omega_t\hat{t}(\theta)}\left|(p+S)\hat{\omega}_t+2\hat{\omega}_{Di}^{(0)}X_{j"}\right|^{-1}$$

$$X_{j"}^2 e^{-X_{j"}^2}(\omega-\omega_{*i}[1+\eta_i(X_{j"}^2-3/2)]$$

$$\times J_o^2[(2b_{i\theta}\Lambda)^{1/2}X_{j"}] \quad , \tag{25}$$

where the $X_{j"}$ are the roots of the polynomial

$$\omega-\hat{\omega}_{Di}^{(o)}X^2-(p+S)\hat{\omega}_t X = 0 \quad . \tag{26}$$

III. INTEGRO_DIFFERENTIAL EQUATION AND SOLUTION METHOD

Since the dissipative trapped-electron mode has wavelength long compared to the Debye length, the appropriate normal mode equation is just the quasi-neutrality condition $\sum_j e_j \tilde{n}_j = 0$, or

$$\tilde{n}_e = \tilde{n}_i = \tilde{n}_i^{NR} + \tilde{n}_i^{R} , \tag{27}$$

where $\tilde{n}_e$, $\tilde{n}_i^{NR}$, and $\tilde{n}_i^{R}$ are given by Eqs. (20), (24) and (25) respectively. This general integro-differential equation contains information about several different radial length scales, specifically about variation over the length scale of the spacing of mode rational surfaces Δr_s and over the equilibrium length scale r_n. For realistic parameters for the mode with $(q'r/q) \sim 1$, $\Delta r_s \ll r_n$. This fact may be exploited by making a multiple radial length scale expansion of Eq. (27) in the parameter $\Delta r_s/r_n$ and treating only the lowest order equation in the hierarchy of equations that results. This is equivalent to taking all of the radial equilibrium gradients to be constant in Eq. (27), so that the effects of the real variation of n, T_i, T_e, and q over the tokamak cross-section are simplified. With this approximation, $b_{ir} = -(\rho_i^2/2)\partial^2/\partial r^2 \simeq -(\rho_i^2/2\Delta r_s^2)(\partial^2/\partial S^2)$, and only the <u>explicit</u> S-dependence in $\tilde{n}_e$, $\tilde{n}_i^{NR}$, and $\tilde{n}_i^{R}$ is to be considered in solving the integro-differential equation. Making the abbreviations

$$A \equiv \left[\left(\frac{T_e}{T_i}+\frac{\omega_{*e}}{\omega}\right)(I_1-I_o)-\eta_i\frac{\omega_{*e}}{\omega}[I_o+2b_{i\theta}(I_1-I_o)]\right.$$

$$+\left(\frac{T_e}{T_i}+\frac{\omega_{*e}}{\omega}\right)\left(\frac{\bar{\omega}_{Di}\cos\theta}{\omega}\right)[I_o(2b_{i\theta}-3)+I_1(2-2b_{i\theta})]$$

$$+\eta_i\frac{\omega_{*e}}{\omega}\left(\frac{\bar{\omega}_{Di}\cos\theta}{\omega}\right)[I_o(-6+11b_{i\theta}-4b_{i\theta}^2)$$

$$\left.+I_1(2-9b_{i\theta}+4b_{i\theta}^2)\right]\exp(-b_{i\theta})\frac{\rho_i^2}{2(\Delta r_s)^2}, \qquad (28)$$

$$B \equiv \left[\left(\frac{T_e}{T_i}+\frac{\omega_{*e}}{\omega}\right)I_o+\eta_i\frac{\omega_{*e}}{\omega}[I_o+b_{i\theta}(I_1-I_o)]\right]\exp(-b_{i\theta})\frac{\bar{\omega}_{ti}^2}{2\omega^2}, \qquad (29)$$

$$C \equiv 1+\frac{T_e}{T_i}-\left(\frac{T_e}{T_i}+\frac{\omega_{*e}}{\omega}\right)I_o\exp(-b_{i\theta})-\eta_i\frac{\omega_{*e}}{\omega}b_{i\theta}(I_1-I_o)\exp(-b_{i\theta}), \qquad (30)$$

$$D \equiv -\left(\frac{T_e}{T_i}+\frac{\omega_{*e}}{\omega}\right)\left(\frac{\bar{\omega}_{Di}\cos\theta}{\omega}\right)[I_o(2-b_{i\theta})+I_1b_{i\theta}]\exp(-b_{i\theta})$$

$$-\eta_i\frac{\omega_{*e}}{\omega}\left(\frac{\bar{\omega}_{Di}\cos\theta}{\omega}\right)[I_o(2-4b_{i\theta}+2b_{i\theta}^2)+I_1(3b_{i\theta}-2b_{i\theta}^2)]\exp(-b_{i\theta})$$

$$-\left(\frac{T_e}{T_i}+\frac{\omega_{*e}}{\omega}\right)\left(\frac{\bar{\omega}_{Di}\cos\theta}{\omega}\right)^2[I_o(7-6b_{i0}+2b_{i0}^2)+I_1$$

$$\cdot(5b_{i\theta}-2b_{i\theta}^2)]\exp(-b_{i\theta})-\eta_i\frac{\omega_{*e}}{\omega}\frac{\bar{\omega}_{Di}\cos\theta}{\omega}[I_o(14-25b_{i\theta}$$

$$+19b_{i\theta}^2-4b_{i\theta}^3)+I_1(17b_{i\theta}-17b_{i\theta}^2+4b_{i\theta}^3)]\exp(-b_{i\theta}), \qquad (31)$$

$$E \equiv -\left[\left(\frac{T_e}{T_i}+\frac{\omega_{*e}}{\omega}\right)[2(I_o-I_1)+I_1/b_{i\theta}]+\eta_i\frac{\omega_{*e}}{\omega}\right.$$

$$\left.\cdot[3I_o-I_1+4b_{i\theta}(I_o-I_1)]\right]\exp(-b_{i\theta})\frac{\rho_i^4}{8(\Delta r_s)^4}, \qquad (32)$$

$$K^{1}\tilde{\phi} \equiv -\frac{2}{\pi^{1/2}} \int_{1-\epsilon_o}^{h(\theta)} d\Lambda \frac{\tilde{\phi}^{(o)}(\Lambda,S,\theta)}{h(\theta)[1-\Lambda/h(\theta)]^{1/2}}$$

$$\int_{o}^{\infty} dX\, X^2\, e^{-X^2} \frac{\omega - \omega_{*e}[1+\eta_e(X^2-3/2)]}{\omega + i(\nu_e/\epsilon_o)X^{-3} - \hat{\omega}_{De}^{(o)} X^2}\ , \qquad (33)$$

$$K^{2}\tilde{\phi} \equiv i\pi^{1/2} \int_{o}^{1-\epsilon_o} d\Lambda \frac{1}{h(\theta)[1-\Lambda/h(\theta)]^{1/2}} \sum_{p=-\infty}^{\infty} \sum_{j"=1}^{2} \sum_{\sigma_{||}=\pm 1} H(X_{j"}^2)$$

$$\cdot \tilde{\phi}^{(p)}(\Lambda,S,\theta) X_{j"}^2 \exp(-X_{j"}^2) \left| (p+S)\hat{\omega}_t + 2\hat{\omega}_{Di}^{(o)} X_{j"} \right|^{-1}$$

$$\cdot \exp[ip\omega_t \hat{t}(\theta)]\, J_o^2[(2b_{i\theta}\Lambda)^{1/2} X_{j"}] \left(\omega - \omega_{*i}[1+\eta_i(X_{j"}^2 - \tfrac{3}{2})]\right), \qquad (34)$$

and

$$K^{3}\tilde{\phi} \equiv i\pi^{1/2} \int_{o}^{1-\epsilon_o} d\Lambda \frac{1}{h(\theta)[1-\Lambda/h(\theta)]^{1/2}} \sum_{p=-\infty}^{\infty} \sum_{j"=1}^{5} \sum_{\sigma_{||}=\pm 1} H(X_{j"}^2)$$

$$\cdot \tilde{\phi}^{(p)}(\Lambda,S,\theta) X_{j"}^2 \exp(-X_{j"}^2) \left| (p+S)\hat{\omega}_t + 3i(\nu_e/\epsilon_o) X_{j"}^{-4} \right.$$

$$\left. + 2\hat{\omega}_{De}^{(o)} X_{j"} \right|^{-1} \left(\omega - \omega_{*e}[1+\eta_e(X_{j"}^2 - 3/2)]\right) \exp[ip\omega_t \hat{t}(\theta)], \qquad (35)$$

the integro-differential equation can be written as

$$0 = \left[A(\theta)\frac{\partial^2}{\partial S^2} + B\left(\frac{\partial}{\partial\theta} + iS\right)^2 + C + D(\theta) + E\frac{\partial^4}{\partial S^4}\right]\tilde{\phi}(\theta,S) + K^{1}\tilde{\phi} + K^{2}\tilde{\phi} + K^{3}\tilde{\phi}\ , \qquad (36)$$

or, as

$$0 = L\tilde{\phi}\ , \qquad (37)$$

where L is an integro-differential operator.

In order to solve Eq. (37), in which L is a complex, linear, non-Hermitian integro-differential operator, $\tilde{\phi}(\theta,S)$ is expanded in complete sets of basis functions in both the S and θ directions, thus converting the integro-differential equation into a matrix equation. Specifically,

$$\tilde{\phi}(\theta,S) = \sum_{n=o}^{\infty} \sum_{j=-\infty}^{\infty} \tilde{\phi}_{jn} g_j(\theta) h_n(S) \ , \tag{38}$$

where the $g_j(\theta)$ and the $h_n(S)$ may be chosen for numerical efficiency, but must be complete, orthonormal sets of functions, with the $g_j(\theta)$ being periodic with period 2π, and the $h_n(S)$ satisfying the boundary conditions, which will be left indefinite for now. Note that Eq. (38) does not involve any assumption of separability. Hence the $g_j(\theta)$ and $h_n(S)$ have the properties

$$\int_{-\pi}^{\pi} d\theta \, g_j(\theta) g_{j'}^*(\theta) = \delta_{jj'} \ , \tag{39}$$

and

$$\int dS \, h_n(S) h_{n'}(S) = \delta_{nn'} \ . \tag{40}$$

Equation (37) now becomes

$$0 = \sum_{j,n} \tilde{\phi}_{j,n} L g_j(\theta) h_n(S) \ , \tag{41}$$

so that

$$0 = \int_{-\pi}^{\pi} d\theta \int dS\, g^{*}_{j',}(\theta) h_{n',}(S) \sum_{j,n} \tilde{\phi}_{j,n} L\, g_j(\theta) h_n(S) = \sum_{j,n} \tilde{\phi}_{j,n} L_{jj',nn'} , \tag{42}$$

which is the desired matrix equation with

$$L_{jj',nn'} \equiv \int_{-\pi}^{\pi} d\theta \int dS\, g^{*}_{j',}(\theta) h_{n',}(S)\, L\, g_j(\theta) h_n(S) . \tag{43}$$

This can be broken up into terms corresponding to the terms in Eq. (36), namely

$$L_{jj',nn'} \equiv A_{jj',nn'} + B_{jj',nn'} + C\delta_{jj'}\delta_{nn'} + D_{jj',nn'} + E_{jj',nn'} + K^{1}_{jj',nn'} + K^{2}_{jj',nn'} + K^{3}_{jj',nn'} . \tag{44}$$

The quantity to be considered as the "eigenvalue" is just the constant complex quantity $(-C)$, since

$$\sum_{j,n} (L_{jj',nn'} - C\delta_{jj'}\delta_{nn'})\tilde{\phi}_{jn} = -C\tilde{\phi}_{j'n'} . \tag{45}$$

Since the frequency ω enters Eq. (37) in a complicated fashion, an approximate value ω_o for the frequency can be "corrected" by a frequency shift $\delta\omega \equiv \omega - \omega_o < \omega_o$ obtained from a perturbation expansion. Thus, ω can be obtained recursively, starting with an initial guess obtained, for instance, from a "local" numerical code for the dissipative trapped-electron mode.[8] Considering only the lowest order terms

in $\epsilon_o^{1/2}$ and α in Eq. (36), and expanding to first order in $\delta\omega/\omega_o$, the result for $\delta\omega$ is

$$\frac{\delta\omega}{\omega_{*e}} = -\left(\frac{\omega_o}{\omega_{*e}}\right)^2 \frac{(-\hat{C}) + C(\omega=\omega_o)}{[I_o + \eta_i b_{i\theta}(I_1 - I_o)]\exp(-b_{i\theta})} , \qquad (46)$$

where $(-\hat{C})$ is the eigenvalue for the considered of the matrix $(L_{jj',nn'} - C\delta_{jj'}\delta_{nn'})|_{\omega=\omega_o}$.

To be more specific, the choices which will be made for $g_j(\theta)$ and $h_n(S)$ are

$$g_j(\theta) = (2\pi)^{-1/2}\exp(ij\theta) , \qquad (47)$$

a Fourier series, and

$$h_n(S) = H_n(\sigma^{1/2}S)\exp(-\sigma S^2/2)\, M_n^{-1/2} , \qquad (48)$$

a Hermite function series, where H_n denotes a Hermite polynomial and $M_n \equiv (\pi/\sigma)^{1/2}2^n n!$. Here σ is a parameter [with $\mathrm{Re}(\sigma) > 0$] which can be adjusted to minimize the number of radial basis functions which need to be retained. Note that σ need not be the value which would be calculated from Weber's equation.[9] In what follows, calculations using Weber's equation will be referred to as local. Considering that the equation to be solved is the lowest in a hierarchy in $(\Delta r_s/r_n)$, the limits of the S integration may be extended from those corresponding to the magnetic axis and the limiter to $\pm\infty$, (or more specifically, $\pm\infty \cdot \sigma^{-1/2}$). The boundary conditions to be imposed are $\tilde{\phi} \to 0$ as $S \to \pm\infty$, which are automatically satisfied for $\mathrm{Re}(\sigma) > 0$. This corresponds to "globally" localized modes which may spread

over a number of mode-rational surfaces, and to outgoing energy at $S \to \pm\infty$.

Using the expressions in Eqs. (47) and (48) for the basis functions, some of the terms in Eq. (44) can be computed analytically. Using the differentiation and recursion relations for Hermite functions[10] gives

$$\frac{\partial^2}{\partial S^2}[H_n(\sigma^{1/2}S)\exp(-\sigma S^2/2)] = \sigma[\tfrac{1}{4}H_{n+2} - (n+\tfrac{1}{2})H_n + n(n-1)H_{n-2}]\exp(-\sigma S^2/2). \quad (49)$$

Using Eq. (49) and simple trigonometric identities gives

$$\begin{aligned} A_{jj',nn'} = \Bigg\{ & \delta_{jj'}\left[-\left(\frac{T_e}{T_i}+\frac{\omega_{*e}}{\omega}\right)(I_o-I_1) - \eta_i \frac{\omega_{*e}}{\omega}[I_o + b_{i\theta}(I_1 - I_o)]\right] \\ & + \frac{\bar{\omega}_{Di}}{2\omega}(\delta_{j+1,j'} + \delta_{j-1,j'})\left[\left(\frac{T_e}{T_i}+\frac{\omega_{*e}}{\omega}\right)[I_o(2b_{i\theta}-3) \right. \\ & \left. + I_1(2-2b_{i\theta})] + \eta_i \frac{\omega_{*e}}{\omega}[I_o(-6+11b_{i\theta}-4b_{i\theta}^2) \right. \\ & \left. + I_1(2-9b_{i\theta}+4b_{i\theta}^2)]\right]\Bigg\} \exp(-b_{i\theta})\frac{\rho_i^2}{2(\Delta r_s)^2}\sigma\left[-(n+\tfrac{1}{2})\delta_{nn'} \right. \\ & \left. + n(n-1)\left(\frac{M_{n-2}}{M_n}\right)^{1/2}\delta_{n-2,n'} + \frac{1}{4}\left(\frac{M_{n+2}}{M_n}\right)^{1/2}\delta_{n+2,n'}\right]. \end{aligned} \quad (50)$$

The recursion relation for Hermite functions then gives

$$B_{jj',nn'} = B\delta_{jj'}\Big[\delta_{nn'}\left[-j^2 - \left(n+\tfrac{1}{2}\right)\tfrac{1}{\sigma}\right]$$

$$+ \delta_{n-1,n'}\left(-j\,\frac{2n}{\sigma^{1/2}}\right)\left(\frac{M_{n-1}}{M_n}\right)^{1/2}$$

$$+ \delta_{n+1,n'}\left(-j\,\frac{1}{\sigma^{1/2}}\right)\left(\frac{M_{n+1}}{M_n}\right)^{1/2}$$

$$+ \delta_{n-2,n'}\left(-\frac{n(n-1)}{\sigma}\right)\left(\frac{M_{n-2}}{M_n}\right)^{1/2}$$

$$+ \delta_{n+2,n'}\left(\frac{-1}{4\sigma}\right)\left(\frac{M_{n+2}}{M_n}\right)^{1/2}\Big] \qquad (51)$$

Also

$$D_{jj',nn'} = -\delta_{nn'}(\delta_{j+1,j'} + \delta_{j-1,j'})\frac{\bar{\omega}_{Di}}{2\omega}\left[\left(\frac{T_e}{T_i} + \frac{\omega_{*e}}{\omega}\right)[I_o(2 - b_{i\theta})\right.$$

$$\left. + I_1 b_{i\theta}] + \eta_i\,\frac{\omega_{*e}}{\omega}[I_o(2 - 4b_{i\theta} + 2b_{i\theta}^2) + I_1(3b_{i\theta} - 2b_{i\theta}^2)]\right]$$

$$\cdot \exp(-b_{i\theta}) - \delta_{nn'}(\delta_{jj'} + \tfrac{1}{2}\delta_{j+2,j'}$$

$$+ \tfrac{1}{2}\delta_{j-2,j'})\frac{\bar{\omega}_{Di}^2}{2\omega^2}\left[\left(\frac{T_e}{T_i} + \frac{\omega_{*e}}{\omega}\right)[I_o(7 - 6b_{i\theta} + 2b_{i\theta}^2)\right.$$

$$+ I_1(5b_{i\theta} - 2b_{i\theta}^2)] + \eta_i\,\frac{\omega_{*e}}{\omega}[I_o(14 - 25b_{i\theta} + 19b_{i\theta}^2 - 4b_{i\theta}^3)$$

$$\left. + I_1(17b_{i\theta} - 17b_{i\theta}^2 + 4b_{i\theta}^3)]\right]\exp(-b_{i\theta}) , \qquad (52)$$

and

$$E_{jj',nn'} = \delta_{jj'} E\sigma^2 \Big\{ \delta_{nn'} \left(\frac{3}{2} n^2 + \frac{3}{2} n + \frac{3}{4}\right) + \delta_{n-2,n'} \left[-(2n-1)n(n-1)\right] \cdot \left(\frac{M_{n-2}}{M_n}\right)^{1/2} + \delta_{n+2,n'} \left[\left(\frac{1}{2} n + \frac{3}{4}\right) \left(\frac{M_{n+2}}{M_n}\right)^{1/2} \right] + \delta_{n-4,n'} \left[n(n-1)(n-2)(n-3)\right] \left(\frac{M_{n-4}}{M_n}\right)^{1/2} + \delta_{n+4,n'} \frac{1}{16} \left(\frac{M_{n+4}}{M_n}\right)^{1/2} \Big\} . \tag{53}$$

The integral terms $K^1\tilde{\phi}$, $K^2\tilde{\phi}$, and $K^3\tilde{\phi}$ are put into computationally convenient forms in Appendix C.

IV. NUMERICAL RESULTS

Six different cases have been investigated with the computer code which implements the procedure described in the preceding section. The chosen and derived parameters for these cases are given in Table I. In Table I, ν_e^* is defined as $\nu_e/(\epsilon_0^{3/2}\bar{\omega}_{te})$. The perturbed electrostatic potential for Case (a) is reasonably localized radially, allowing comparison to previous Weber's equation solutions for the radial dependence.[3,8] Case (b) is set up to allow comparison with previous results for the poloidal dependence.[1,2] The parameters of Case (c) are chosen such that the expansion for $k_r\rho_i < 1$ just breaks down, so that a limit for the region of validity in parameter space for the present formalism can be ascertained. Case (d) is a basic case of practical interest, for which a $k_r\rho_i < 1$ expansion converges properly. It has been run with different terms in Eq. (44) turned on and off, to allow assessment of their individual effects. Case (e) differs from Case (d) only in the assumed aspect ratio, to investigate the effects of varying this parameter. Likewise, Case (f) differs from Case (d) only in choosing opposite signs for the density and temperature gradients in order to study this stabilizing effect[4] in the context of a nonlocal calculation.

The final results for $\omega = \omega_r + i\gamma$ and $\sigma = \sigma_r + i\sigma_i$ for the six cases are given in Table II. These results are obtained with all of the terms in Eq. (44) included, except for Case (b) (see below). Only results for the lowest eigenmode, that is, the one with the least number of radial and poloidal nodes, are given for each case. This is generally seen to be the eigenmode corresponding to the largest growth rate, and is therefore of most interest.

It should be noted here that previous one-dimensional studies[1,3] also indicate this basic trend; i.e., the lowest eigenmodes have the largest growth rates. Higher eigenmodes can be investigated by the two-dimensional code, but this will be left for future investigation. The general procedure was to choose a value for σ and then to compute the value of ω recursively with Eq. (46) until it converged for the lowest eigenmode. The value of σ is then varied to get the best convergence of the coefficients of the radial basis functions. The value of ω is computed recursively again until it converges on a final value. The final results presented in Table II are generally for eleven radial basis functions ($n = 0$ through 10), seven poloidal basis functions ($j = -3$ through 3), and eleven transit frequency harmonics in the resonance terms ($p = -5$ through 5), except as noted below. This means that it was necessary to numerically solve a (77×77) matrix for the eigenfunction. Plots of the final lowest eigenfunctions for the six cases considered are shown in Figs. 1 through 6. For Cases (a), (c), (d), (e), and (f) these are three-dimensional plots of the real and imaginary parts of $\tilde{\phi}(\theta,S)$. Only positive values of S are shown, since the lowest eigenfunction is always symmetric in $(S\theta)$. Higher eigenfunctions can be either even or odd in $(S\theta)$. In Table II, results for ω and σ obtained from the local code of Ref. 8 are also given. Here the value of σ obtained by solving Weber's equation is just[9]

$$\sigma_\ell = \left(\frac{T_e}{T_i}\,\frac{q'r}{q}\,b_{i\theta}\right)^{-1}\,\frac{r_n}{r}\,\frac{\epsilon_o}{q}\,\frac{\omega_{*e}}{\omega_r^2+\gamma^2}\,(\gamma + i\omega_r)\ . \tag{54}$$

However, to make the comparison between the local and the two-dimensional results more meaningful, the first and second order ion magnetic drift terms, as given in Eq. (23), have been added to the local code. Also added was the Weber's equation correction to the dispersion relation (shear-dependent convective term) which was derived in Ref. 8, but was only used to determine marginal stability conditions there. Note that all of the frequencies presented in Table II are in units of ω_{*e}, so that physical frequencies and growth rates are proportional to the numbers listed multiplied by $b_{i\theta}^{1/2}$.

For Case (a), the parameters are chosen so that comparison is possible to a radial one-dimensional analysis[3] which applies to the dissipative trapped-electron mode a method first used by Pearlstein and Berk[11] for the "universal" electron drift mode. The calculation in Ref. 3 includes only the first radial finite ion Larmor radius correction term, the ion sound term, and the spatially constant terms, with no poloidal dependence. These correspond to the A, B, C, and K^1 terms in Eq. (44). Therefore, the other terms and the poloidal dependence have been suppressed in the two-dimensional code in making the comparison. The solutions of the Weber's equation obtained in Ref. 3 are just the Hermite functions used as basis functions for the two-dimensional calculation, if σ is taken equal to σ_ℓ, with σ_ℓ computed from Eq. (54) using the values of ω_r and γ obtained from the local code[8] with the corresponding terms suppressed. A "radial diagonal dominance index" is defined as the sum of the absolute squares of all the radially off-diagonal ($n' \neq n$) elements

of the $(L_{jj',nn'} - C\delta_{jj'}\delta_{nn'})$ matrix divided by the sum of the absolute squares of all the radially diagonal ($n = n'$) elements. This index was computed as the real and imaginary parts of σ were varied, keeping the first five Hermite functions in the basis, and was found to be a minimum when $\sigma = \sigma_\ell$. This means that the set of numerically computed eigenfunctions was closest to the set of Hermite function solutions of Weber's equation when $\sigma = \sigma_\ell$, as would be expected for a mode localized around one mode-rational surface. It thus constitutes a check of consistency between the two-dimensional computation and a previous one-dimensional calculation, for parameters such that the latter is expected to be a reasonable approximation. Note that this was with the poloidal dependence suppressed; when this dependence was included, the value of σ which minimized the index shifted significantly from σ_ℓ. Also note that the index is useful only for global comparisons of all the radial eigenmodes; it is not particularly useful for testing the convergence of the coefficients for any single eigenfunction.

Another check of the two-dimensional code was performed using the parameters of Case (a). To verify that the eigenfunction obtained is reasonably independent of the choice of σ, the final eigenfunctions for Case (a), including all terms, were recomputed for two other values of σ. The lowest eigenfunction, as measured by the S-values of the zeroes of its theta-average, changed by about 12% for a 20% reduction in σ and by about 15% for a 40% reduction. These changes in the eigenfunction are of the same order as the inverse of the

number of radial basis functions used, that is 9% for 11 Hermite functions. Thus the accuracy obtained is about what would be expected.

The parameters of Case (b) are chosen to allow comparison with previous one-dimensional analyses of the mode structure along a field line.[1,2] For a one-dimensional integral equation which would correspond to Eq. (36) with only the C and K^1 terms retained, for $b_i \ll 1$, a result close to $\tilde{\phi}(\theta) \propto \cos^2(\theta/2) \propto (1+\cos\theta)$ was obtained. In running Case (b) only the corresponding terms were retained. The result for $\tilde{\phi}(\theta, S=0)$, shown in Fig. 2, is also similar to $(1+\cos\theta)$. This constitutes another check of the two-dimensional calculation against a previous one-dimensional analytic result. The entries in Table II for Case (b) reflect only the retained C and K^1 terms. This simple $(1+\cos\theta)$ dependence will, of course, be modified by the omitted terms, in particular by the ion sound and ion curvature drift terms.

Case (c) has been used to test the limit of validity of the $b_{ir} = -(\rho_i^2/\Delta r_s^2)(\partial^2/\partial S^2) < 1$ assumption that has been made. In particular, the limit on $b_{i\theta}$ that this implies is checked a posteriori. Estimating the maximum value of $(\partial^2\tilde{\phi}/\partial S^2)/\tilde{\phi}$ from Fig. 3 indicates that $b_{ir} \sim 2$, so that $b_{ir}/b_{i\theta} \sim 20$. Thus the $b_{ir} < 1$ assumption has broken down, and the Case (c) results are really only an extrapolation of the $b_{ir} < 1$ formulation, somewhat beyond its range of validity. If $b_{ir}/b_{i\theta} \sim 10$ to 20, as is also indicated by the results for Case (d), then the limit on $b_{i\theta}$ is $b_{i\theta} \lesssim 0.05$, and on k_θ is $k_\theta \rho_i \lesssim 0.3$. Treating larger

values of $b_{i\theta}$ would thus require a more general formulation for treating finite ion Larmor radius effects, specifically an integral instead of a differential method. This generalization is currently under investigation.

For Case (d), $b_{i\theta} = 0.025$ and, as can be verified from Fig. 4, $b_{ir} < 1$ here. For the parameters of Case (d), the effects on ω of turning on and off the various terms in Eq. (44) are given in Table III. Comparing the results, it may be seen that the ion sound term, the B term in Eq. (44), is substantially stabilizing. This is expected since this is the term which is mainly responsible for energy convection away from the radial region where the mode is localized. The first order ion magnetic drift term, which is part of the E term in Eq. (44), causes a large decrease in ω_r, which has a stabilizing effect in this instance. Results from the local code also exhibit this behavior. The second order ion magnetic drift term, the other part of the E term in Eq. (44), serves to partially reverse the effects of the first order term. This trend again corresponds to results from the local code. As expected, the ion resonance term, the K^2 term in Eq. (44), is somewhat stabilizing. The electron resonance term, the K^3 term in Eq. (44), is also somewhat stabilizing, which indicates that the effect of energy absorption at mode-rational surfaces is stronger than the effect of energy reflection there.

The only chosen parameter in Case (e) which differs from Case (d) is the inverse aspect ratio ϵ_0. It is seen that the effect of decreasing ϵ_0 from 0.25 to 0.12 is destabilizing in its

net effect on the mode. The same behavior is seen in the results from the local code. This trend will, of course, not continue as ϵ_o approaches zero, since the main destabilizing term, the trapped electron time-average term, would thereby be eliminated; thus this observed destabilization should not be generalized indiscriminately.

Case (f) differs from Case (d) only in the signs of η_i and η_e. This change was seen to be strongly stabilizing in local calculations,[4,8] and it remains so in this two-dimensional calculation. Hence, an equilibrium situation with oppositely directed density and temperature gradients is more favorable in terms of dissipative trapped-electron mode stability.

V. CONCLUSIONS

As pointed out in the preceding discussion of Cases (a) and (b), the present two-dimensional calculation can reproduce characteristic features of previous one-dimensional analytic solutions in limits for which these one-dimensional solutions are expected to be valid. Also the solution method for the two-dimensional integro-differential equation permits the treatment of cases such as (c), (d), (e), and (f), for which previous solutions are invalid. It allows examination of the results of the interaction of different terms, and of the radial and poloidal dependences of the potential, which would not be possible with a simple perturbation approach.

Certain conclusions about the effectiveness of shear stabilization can be drawn from the results presented in Table II. For Case (a), which is illustrated in Fig. 1, the mode overlaps the mode-rational surfaces at $|S| = 1$ strongly, but not those at larger values of $|S|$. The growth rate from the two-dimensional calculation is much less than predicted by the Weber's equation solution, implemented in the local code. Thus the $|S| = 1$ mode-rational surfaces cause a substantial change in the growth rate. A possible explanation of this behavior is that energy absorption, which tends to decrease the growth rate, dominates over energy reflection, which would tend to increase the growth rate. These effects enter mainly through the circulating-electron resonance term. For Cases (c), (d), (e), and (f), where the modes overlap more mode-rational surfaces, the differences between the local and two-dimensional growth rates are much smaller. Here a possible explanation is that the large number of mode-rational surfaces

overlapped by the mode tend to cancel one another out in their net effect on the growth rate. This is consistent with the smallness of the electron resonance term for Case (d), as is seen in Table III. Then the dominant remaining effect is the convection of energy, because of the ion-sound term, which is included in both the local and two-dimensional results. Thus, the local code, with the Weber's equation solution correction to the dispersion relation, is in fact more accurate in estimating shear stabilization than might be expected. However, Fig. 4, for example, shows that the actual mode structure is quite different. Note that, in general, the local code predicts that the amount of magnetic shear in real tokamaks will be <u>insufficient</u> to stabilize the dissipative trapped-electron mode for normal gradients, and the two-dimensional results confirm this. For oppositely directed temperature and density gradients, however, both codes predict that realistic amounts of shear can stabilize this mode.

The most important limitation on the present analysis is the requirement that $b_{ir} \equiv k_r^2 \rho_i^2/2 < 1$. The results presented in the preceding section indicate that generally $b_{ir}/b_{i0} \equiv b_{ir}/(k_\theta^2 \rho_i^2/2) \simeq 10$ to 20 . The local code predicts that the maximum growth rates will occur for $b_{i\theta} \simeq 0.5$ to 1.0 or even more.[8] Thus, the most interesting part of parameter space is, in fact, inaccessible to the present code. To reach this part of parameter space will require the abandonment of the simple differential formulation of the finite ion Larmor radius effects employed here, for a formulation valid for larger b_{ir} . This problem is currently under investigation. The present integro-differential equation and its

solution method nevertheless represent a substantial improvement over previous studies of the spatial structure of this mode. It is anticipated that other improvements, such as the inclusion in the integro-differential equation of some terms omitted here, the use of a more accurate electron collision operator, and the addition of ion collisional effects will also be incorporated in future work. This should allow study of the mode for higher collisionalities, which are relevant for interpreting the experimental results from present machines.

ACKNOWLEDGMENTS

This work was supported by U.S. Energy Research and Development Administration Contract E(11-1)-3073.

APPENDIX A

The linearized drift kinetic equation (for a magnetic field independent of time), in terms of the quantities defined in Section II, is

$$[\frac{\partial}{\partial t} + (\underset{\sim}{v}_{||} + \underset{\sim}{v}_B) \cdot \nabla] f_e^{(1)} = - \underset{\sim}{v}_E^{(1)} \cdot \nabla f_e^{(o)} - e(\underset{\sim}{v}_{||} + \underset{\sim}{v}_B) \cdot \nabla\tilde{\Phi} \times \frac{\partial f_e^{(o)}}{\partial t} - \nu_f(\varepsilon)[f_e^{(1)} - (e\tilde{\Phi}/T_e) f_{Me}] \quad , \quad (A1)$$

where $f_e^{(1)}$ is the perturbed electron distribution function, $\underset{\sim}{v}_E^{(1)}$ is the perturbed electric drift velocity, and $\underset{\sim}{v}_B$ is the magnetic drift velocity. Using the assumed form for $f_e^{(o)}$ gives

$$\left.\frac{df_e^{(1)}}{dt}\right|_b \equiv [\frac{\partial}{\partial t} + (\underset{\sim}{v}_{||} + \underset{\sim}{v}_B) \cdot \nabla] f_e^{(1)}$$

$$= \frac{e}{T_e} (\underset{\sim}{v}_{||} + \underset{\sim}{v}_B) \cdot \nabla\tilde{\Phi} f_{Me} - \frac{e}{\Omega_{\theta e}} (\underset{\sim}{v}_{||} + \underset{\sim}{v}_B) \cdot \nabla\tilde{\Phi}\left(\frac{v_{||}}{T_e} - \frac{1}{m_e v_{||}}\right)$$

$$\times \frac{\partial f_{Me}}{\partial r} - \underset{\sim}{v}_E^{(1)} \cdot \nabla f_e^{(o)} - \nu_f[f_e^{(1)} - (e\tilde{\Phi}/T_e) f_{Me}] \quad , \quad (A2)$$

where

$$\frac{\partial f_{Me}}{\partial r} = f_{Me} [\frac{1}{n}\frac{dn}{dr} - \frac{1}{T_e}\frac{dT_e}{dr}(\frac{3}{2} - \frac{\varepsilon}{T_e})] \quad (A3)$$

and $(d/dt)\big|_b$ indicates the total derivative along a guiding-center (banana) orbit. Note that $v_B/v_{||} = O(\rho_i/R_o)$, so that $\underset{\sim}{v}_B$ can be neglected relative to $\underset{\sim}{v}_{||}$. Also $(v_{||}/T_e)$ is smaller by one order in ϵ_o than $1/(m_e v_{||})$ for the trapped and barely circulating particles which are of most interest. Thus we have

$$\left.\frac{df_e^{(1)}}{dt}\right|_b \simeq \frac{e}{T_e} f_{Me} \left(\left.\frac{d}{dt}\right|_b - \frac{\partial}{\partial t} + \nu_f\right) \tilde{\Phi}$$

$$- \left[\frac{-|e|}{m_e \Omega_{\theta e}} \nabla_{||} \tilde{\Phi} + v_{Er}^{(1)}\right] \cdot \frac{\partial f_{Me}}{\partial r} - \nu_f f_e^{(1)}$$

$$\simeq \frac{e}{T_e} f_{Me} \left(\left.\frac{d}{dt}\right|_b + i\omega + \nu_f\right) \tilde{\Phi}$$

$$- \frac{c}{RB_\theta} \frac{\partial f_{Me}}{\partial r} \frac{\partial \tilde{\Phi}}{\partial \zeta} - \nu_f f_e^{(1)} \quad , \tag{A4}$$

to lowest order in ϵ_o. Since $\partial\tilde{\Phi}/\partial\zeta = i\ell\tilde{\Phi}$, this may be rewritten as

$$\left(\left.\frac{d}{dt}\right|_b + \nu_f\right) f_e^{(1)} = \frac{e}{T_e} f_{Me} \left[\left(\left.\frac{d}{dt}\right|_b + \nu_f\right) \tilde{\Phi} + i(\omega - \omega_{*e}^T)\tilde{\Phi}\right] \quad , \tag{A5}$$

where the definition

$$\omega_{*e}^T \equiv \omega_{*e}\left[1 + \eta_e\left(\frac{\varepsilon}{T_e} - \frac{3}{2}\right)\right] \tag{A6}$$

has been used. Equation (A5) is equivalent to

$$\left.\frac{d}{dt}\right|_b \left[f_e^{(1)} \exp(\nu_f t)\right] = \frac{e}{T_e} f_{Me} \left[\left.\frac{d}{dt}\right|_b + i(\omega - \omega_{*e}^T)\right] \left[\tilde{\Phi} \exp(\nu_f t)\right] \quad . \tag{A7}$$

Equation (A7) may be integrated along the unperturbed guiding-center orbits to obtain

$$f_e^{(1)} = \frac{ef_{Me}}{T_e} \left[\tilde{\Phi} + i(\omega-\omega_{*e}^T) \exp(-\nu_f t) \int_{-\infty}^{t} dt' \, \tilde{\Phi} \exp(\nu_f t')\right] . \quad (A8)$$

Here t' is the time parameter along the unperturbed orbit, and the integration is subject to the boundary conditions $\theta(t'=t) = \theta$ and $r(t'=t) = r$. Adopting the notation

$$f_e^{(1)} = \tilde{f}_e \exp(-i\omega t + i\ell\zeta - im^o\theta) , \quad (A9)$$

Eq. (A8) can be rewritten as

$$\tilde{f}_e = \frac{ef_{Me}}{T_e} \{\tilde{\phi}(\theta,S) + i(\omega - \omega_{*e}^T) \int_{-\infty}^{t} dt' \tilde{\phi}(\theta',S')$$

$$\times \exp[-i(\omega+i\nu_f)(t'-t)] \exp[i(\ell\zeta'-m^o\theta') - i(\ell\zeta-m^o\theta)]\} , \quad (A10)$$

where the abbreviation $\theta(t') = \theta'$, $r(t') = r'$, $\zeta(t') = \zeta'$, and $S' = S[r(t')]$ have been used.

To do the t' integration, an explicit form is needed for $\ell\zeta' - m^o\theta'$, specifically

$$(\ell\zeta' - m^o\theta') = \ell \int_{t}^{t'} dt'' \left[\frac{d\zeta}{dt''} - q(r_o) \frac{d\theta}{dt''}\right] + (\ell\zeta - m^o\theta) , \quad (A11)$$

recalling that $q(r_o) = m^o/\ell$. Notice that

$$\frac{d\zeta}{dt''} - q(r) \frac{d\theta}{dt''} \equiv \dot{\beta}_{MD} \quad (A12)$$

results from the instantaneous magnetic (gradient and curvature) drift velocity v_{MD} of the guiding center, so that

$$(\ell\zeta' - m^o\theta') = \ell\{q[r^{(o)}] - q(r_o)\}(\theta' - \theta) + \int_t^{t'} dt'' \, \omega_{De}(t'') + (\ell\zeta - m^o\theta) \quad , \tag{A13}$$

where

$$\omega_{De} \equiv \ell\left(\dot{\beta}_{MD} + \{q(r) - q[r^{(o)}]\}\frac{d\theta}{dt''}\right) \tag{A14}$$

and

$$r^{(o)} \equiv \frac{1}{\tau_{b,t}} \oint dt \, r \tag{A15}$$

is the time average of r along the guiding-center orbit, with $\tau_{b,t}$ equaling τ_b or τ_t as appropriate. Equation A13) becomes

$$(\ell\zeta' - m^o\theta') - (\ell\zeta - m^o\theta) = S^{(o)}(\theta' - \theta) + \omega_{DE}^{(o)}(t' - t) + w_{De}^{(\sim)} \quad , \tag{A16}$$

with the definitions

$$\varepsilon^{(o)} \equiv \ell[q[r^{(o)}] - q(r_o)] \quad , \tag{A17}$$

$$\omega_{De}^{(o)} \equiv \frac{1}{\tau_{b,t}} \oint dt'' \, \omega_{De}(t'') \quad , \tag{A18}$$

and

$$w_{De}^{(\sim)} \equiv \int_{t}^{t'} dt'' \; [\omega_{De}(t'') - \omega_{De}^{(o)}] \quad . \tag{A19}$$

Then for trapped particles

$$(\ell\zeta' - m^{o}\theta') - (\ell\zeta - m^{o}\theta) = \omega_{De}^{(o)}(t' - t) + P_{b}^{(\sim)}(t') \quad , \tag{A20}$$

where

$$P_{b}^{(\sim)}(t') = S^{(o)}(\theta' - 0) + w_{De}^{(\sim)} \quad , \tag{A21}$$

while for circulating particles

$$(\ell\zeta' - m^{o}\theta'') - (\ell\zeta - m^{o}\theta) = [\omega_{De}^{(o)} + \omega_{t}S^{(o)}](t' - t) + P_{t}^{(\sim)}(t') \quad , \tag{A22}$$

where

$$P_{t}^{(\sim)}(t') = S^{(o)}(\theta' - \theta) - \omega_{t}S^{(o)}(t' - t) + w_{De}^{(\sim)} \quad . \tag{A23}$$

Note that $P_{b}^{(\sim)}(t')$ and $P_{t}^{(\sim)}(t')$ are periodic functions of t' with periods τ_{b} and $|\tau_{t}|$ respectively. Therefore it is useful to employ the decompositions

$$\tilde{\phi}(\theta',S') \exp[iP_{b,t}^{(\sim)}(t')] = \sum_{p=-\infty}^{\infty} \tilde{\Phi}^{(p)} \exp\{ip\omega_{b,t}\hat{t}[0(t')]\} \quad , \tag{A24}$$

where the summation is over all integer values of p, and $P_{b,t}^{(\sim)}$ and $\omega_{b,t}$ mean $P_{b}^{(\sim)}$ and ω_{b} for trapped particles and $P_{t}^{(\sim)}$ and ω_{t} for circulating particles. The parametric function $\hat{t}(\theta)$ is defined by

$$\hat{t}(\theta) \equiv qR_o \int_0^\theta d\theta'/v_{||}(\theta') + \text{constant} \quad , \tag{A25}$$

and the constant can be chosen such that $\hat{t}[\theta(t')] = t'$ over some bounce or transit period of interest. The inversion formula is

$$\tilde{\Phi}^{(p)} = \frac{1}{\tau_{b,t}} \oint dt' \tilde{\phi}(\theta', S') \exp\left[iP^{(\sim)}_{b,t}(t')\right] \exp\left\{-ip\omega_{b,t}\hat{t}[\theta(t')]\right\} \tag{A26}$$

at constant θ. By means of these decompositions the time integration in Eq. (A10) can be done exactly

$$\tilde{f}_e = \frac{ef_{Me}}{T_e}\left(\dot{\phi}(\theta,S) + i(\omega - \omega^T_{*e}) \int_{-\infty}^{t} dt' \sum_p \tilde{\Phi}^{(p)}\right.$$

$$\left. \times \exp\left\{ip\omega_{b,t}\hat{t}[\theta(t')]\right\} \exp\left\{-i\left[\omega + i\nu_f - \omega^{(o)}_{De} - S^{(o)}\omega_t H(\Lambda_c - \Lambda)\right](t'-t)\right\}\right)$$

$$= \frac{ef_{Me}}{T_e}\left(\tilde{\phi}(\theta,S) - (\omega-\omega^T_{*e}) \sum_p \frac{\tilde{\Phi}^{(p)} \exp\left[ip\omega_{b,t}\hat{t}(\theta)\right]}{\omega + i\nu_f - \omega^{(o)}_{De} - \left[p+S^{(o)}H(\Lambda_c-\Lambda)\right]\omega_{b,t}}\right) \tag{A27}$$

where H is the Heaviside step function and $\Lambda_c \equiv 1 - \epsilon_o$, so that $H(\Lambda_c - \Lambda) = 0$ for trapped particles and $H(\Lambda_c - \Lambda) = 1$ for circulating particles. This difference in the form of the denominator in Eq. (A27) reflects the fact that circulating particles sample the entire field line. They are therefore sensitive to the mode-rationality or -irrationality of the magnetic surface on which they move, i.e. to S or $S^{(o)}$. Trapped particles, on the other hand, sample only a part of a field line and are not sensitive to this difference. From the result given in Eq. (A27),

$$\tilde{n}_e \equiv \int d^3 \underset{\sim}{v}\, \tilde{f}_e = \frac{en}{T_e}\left(\tilde{\phi}(\theta,S) - \frac{1}{n}\int d^3 \underset{\sim}{v}\, f_{Me}(\omega-\omega^T_{*e}) \right.$$

$$\left. \times \sum_p \frac{\tilde{\phi}^{(p)} \exp\left[ip\omega_{b,t}\hat{t}(\theta)\right]}{\omega + i\nu_f - \omega^{(o)}_{De} - [p+S^{(o)}H(\Lambda_c-\Lambda)]\omega_{b,t}} \right) \qquad \text{(A28)}$$

This result includes the effects of the electron banana width ρ_{be}. However, for thic problem the dominant radial length is the ion gyroradius ρ_i, which is large compared to ρ_{be} for realistic parameters. Terms of order $S^{(\sim)} \equiv S - S^{(o)}$ can therefore be neqlected. For $(q'r/q)$ of order unity, the quantity $w^{(\sim)}_{De}$ is found to be of the same order, so that it can also be neglected. then $\tilde{n}_e$ becomes

$$\tilde{n}_e = \frac{en}{T_e}\left(\tilde{\phi}(\theta,S) - \frac{\pi}{2n}\left(\frac{2}{m_e}\right)^{3/2} \sum_{\sigma_{||}} \int_0^{h(\theta)} d\Lambda\, \frac{1}{h(\theta)\left[1-\Lambda/h(\theta)\right]^{1/2}} \right.$$

$$\times \int_0^\infty d\varepsilon\, \varepsilon^{1/2} f_{Me}(\varepsilon)\left[\omega-\omega^T_{*e}(\varepsilon)\right] \sum_{p=-\infty}^{\infty} \tilde{\phi}^{(p)}(\Lambda,\theta,S) \exp\left[ip\omega_{b,t}\hat{t}(\theta)\right]$$

$$\left. \times \left\{\omega + i\nu_f(\varepsilon) - \omega^{(o)}_{De}(\Lambda,\varepsilon) - [p + SH(\Lambda_c-\Lambda)]\,\omega_{b,t}(\Lambda,\varepsilon)\right\}^{-1} \right) , \qquad \text{(A29)}$$

where now

$$\tilde{\phi}^{(p)} = \frac{1}{\tau_{b,t}} \oint dt'\, \tilde{\phi}(\theta',r') \exp\left\{iS(\theta'-\theta) - i\omega_t S[\hat{t}(\theta')\right.$$

$$\left. - \hat{t}(\theta)]H(\Lambda_c-\Lambda)\right\} \exp\left\{-ip\omega_{b,t}\hat{t}[\theta(t')]\right\} . \qquad \text{(A30)}$$

In Eq. (A30), if θ is not to be regarded as constant, then dt' is to be interpreted as $dt' = qR_o d(\theta' - \theta)/v_{||}(\theta')$, so that $\tilde{\Phi}^{(p)}(\Lambda,\theta,S)$ will be explicitly periodic in θ.

This result for $\tilde{n}_e$ will now be specialized to the case $\omega, \nu_f, \omega_{De}^{(o)} < \langle\omega_b\rangle_e < \langle\omega_t\rangle_e$, as is appropriate for the dissipative trapped-electron mode in the banana regime, so that the denominators of all the terms may be expanded, except the $p = 0$ (i.e. time average) trapped-electron term. This yields, assuming $\omega_r \equiv \mathrm{Re}(\omega) > \gamma \equiv \mathrm{Im}(\omega)$,

$$\tilde{n}_e \simeq \frac{en}{T_e}\left\{\tilde{\phi}(\theta,S) - \frac{\pi}{2n}\left(\frac{2}{m_e}\right)^{3/2}\frac{1}{h(\theta)}\sum_{\sigma_{||}}\int_0^\infty d\varepsilon\ \varepsilon^{1/2} f_{Me}(\varepsilon)(\omega - \omega_{*e}^T)\right.$$

$$\times\left[\int_{1-\epsilon_o}^{h(\theta)} d\Lambda\ (1-\Lambda/h)^{-1/2}\left(\frac{\tilde{\Phi}^{(o)}}{\omega + i\nu_f - \omega_{De}^{(o)}} - \sum_{p\neq 0}\tilde{\Phi}^{(p)}\exp(ip\omega_b\hat{t})\right.\right.$$

$$\left.\times\left\{\frac{1}{p\omega_b} + \frac{\omega + i\nu_f - \omega_{De}^{(o)}}{p^2\omega_b^2} + i\pi\delta[\omega + i\nu_f - \omega_{De}^{(o)} - p\omega_b]\right\}\right)$$

$$- \int_0^{1-\epsilon_o} d\Lambda\ (1-\Lambda/h)^{-1/2}\sum_p \tilde{\Phi}^{(p)}\exp(ip\omega_t\hat{t})\left\{\frac{1}{(p+S)\omega_t}\right.$$

$$\left.\left.\left.+ \frac{\omega + i\nu_f - \omega_{De}^{(o)}}{(p+S)^2\omega_t^2} + i\pi\delta[\omega + i\nu_f - \omega_{De}^{(o)} - (p+S)\omega_t]\right\}\right]\right\} . \qquad \text{(A31)}$$

Defining $X \equiv (\varepsilon/T_e)^{1/2}$ and using a "hat" (^) to specify that the X dependence has been factored out of a quantity, the trapped-electron delta function can be written as

$$\delta[\omega + i\nu_f(\varepsilon) - \omega_{De}^{(o)}(\Lambda,\varepsilon) - p\omega_b(\Lambda,\varepsilon)]$$

$$= \delta[\omega + i(\nu_e/\epsilon_o)X^{-3} - \hat{\omega}_{De}^{(o)}(\Lambda)X^2 - p\hat{\omega}_b(\Lambda)X]$$

$$= \sum_{j"=1}^{5} \delta(X - X_{j"}) \left| p\hat{\omega}_b + 2\hat{\omega}_{De}^{(o)} X_{j"} + 3i(\nu_e/\epsilon_o) X_{j"}^{-4} \right|^{-1} , \qquad \text{(A32)}$$

where the $X_{j"}$ are the five roots of the polynomial

$$\hat{\omega}_{De}^{(o)}(\Lambda)X^5 + p\hat{\omega}_b(\Lambda)X^4 - \omega X^3 - i(\nu_e/\epsilon_o) = 0 \quad . \qquad \text{(A33)}$$

The result for the circulating-electron delta function term (resonant term) is similar in form.

The interesting terms in Eq. (A31) for the dissipative trapped-electron mode, aside from the $p = 0$ trapped-electron term, are the resonant terms, so the others will be dropped at this point. Using the delta functions to do the ε (or X) integration for the resonant terms gives, finally

$$\tilde{n}_e \simeq \frac{en}{T_e}\left(\tilde{\phi}(\theta,S) - \frac{2}{\pi^{1/2}h}\int_0^{\infty} dX\, X^2 \exp(-X^2)\{\omega - \omega_{*e}[1+\eta_e(X^2-3/2)]\}\right.$$

$$\times \int_{1-\epsilon_o}^{h(\theta)} d\Lambda\,(1-\Lambda/h)^{-1/2}\,\frac{\tilde{\Phi}(o)}{\omega + i(\nu_e/\epsilon_o)X^{-3} - \hat{\omega}_{De}^{(o)}X^2} + i\,\frac{\pi^{1/2}}{h}$$

$$\times \sum_{\sigma_{||}} \int_{1-\epsilon_o}^{h(\theta)} d\Lambda\,(1-\Lambda/h)^{-1/2} \sum_{p\neq 0}\sum_{j''=1}^{5} \exp(ip\omega_b\hat{t})\,\tilde{\Phi}^{(p)}\,H(X_{j''}^2)$$

$$\times \left|p\hat{\omega}_b + 2\hat{\omega}_{De}^{(o)}X_{j''} + 3i(\nu_e/\epsilon_o)X_{j''}^{-4}\right|^{-1} X_{j''}^2 \exp(-X_{j''}^2)$$

$$\times \{\omega - \omega_{*e}[1+\eta_e(X_{j''}^2-3/2)]\} + i\,\frac{\pi^{1/2}}{h}\sum_{\sigma_{||}}\int_0^{1-\epsilon_o} d\Lambda\;(1-\Lambda/h)^{-1/2}$$

$$\times \sum_{p=-\infty}^{\infty}\sum_{j''=1}^{5} \tilde{\Phi}^{(p)}\exp(ip\omega_t\hat{t})\left|(p+S)\hat{\omega}_t + 2\hat{\omega}_{De}^{(o)}X_{j''} + 3i(\nu_e/\epsilon_o)X_{j''}^{-4}\right|^{-1}$$

$$\left.\times X_{j''}^2 \exp(-X_{j''}^2)\{\omega - \omega_{*e}[1+\eta_e(X_{j''}^2-3/2)]\}\right) \quad , \qquad \text{(A34)}$$

where $H(X_{j''}^2) = 0$ for $X_{j''}^2 < 0$ and $H(X_{j''}^2) = 1$ for $X_{j''}^2 \geq 0$. The result (A34) shows that the trapped-electron resonance term does not have the explicit S-dependence of the circulating-electron resonance term. The former is therefore not expected to have any significant effect on the radial structure of the mode, and can thus be neglected.

APPENDIX B

The result for the ions corresponding to Eq. (A28) for the electrons is

$$\tilde{n}_i = -\frac{en}{T_i}\left(\tilde{\phi}(\theta,S) - \frac{1}{n}\int d^3\underset{\sim}{v}\, f_{Mi}(\omega - \omega^T_{*i})J_o^2(k_\perp v_\perp/\Omega_i)\sum_p \right.$$
$$\left. \cdot\, \tilde{\phi}(p)\frac{\exp\,[ip\omega_{b,t}\hat{t}(\theta)]}{\omega + i\nu_f - \omega^{(o)}_{Di} - [p + S^{(o)}H(\Lambda_c - \Lambda)]\omega_{b,t}}\right), \qquad \text{(B1)}$$

with $\omega_{*i} = -(T_i/T_e)\omega_{*e}$ and $\omega_{Di} = -(T_i/T_e)\omega_{De}$. For the ions the relevant frequency ordering is

$$\omega > \omega_{Di}, \langle\omega_{t'i}\rangle \langle\omega_{b'i}\rangle \gtrsim (\nu_i/\cdots). \qquad \text{(B2)}$$

Ion collisional effects are weak for $k_\perp\rho_i \lesssim 1$, and to a good approximation can be neglected.[5] Expanding the denominator then gives

$$\tilde{n}_i \simeq -\frac{en}{T_i}\left[\tilde{\phi}(\theta,S) - \frac{1}{n}\int d^3\underset{\sim}{v}\, f_{Mi}(\omega - \omega^T_{*i})J_o^2\sum_p \tilde{\phi}(p)\right.$$
$$\cdot \exp\,(ip\omega_{b,t}\hat{t})\left(\frac{1}{\omega} + \frac{\omega^{(o)}_{Di} + [p + S^{(o)}H]\omega_{b,t}}{\omega^2}\right.$$
$$+ \frac{\{\omega^{(o)}_{Di} + [p + S^{(o)}H]\omega_{b,t}\}^2}{\omega^3} - i\pi\delta\{\omega - \omega^{(o)}_{Di}$$
$$\left.\left. - [p + S^{(o)}H]\omega_{b,t}\} + \cdots\right)\right]. \qquad \text{(B3)}$$

Sum rules can be derived which make it possible to perform the p summations by the following procedure for circulating

particles. Trapped particles may be treated similarly. The analog of Eq. (A24) is, for circulating ions,

$$\tilde{\phi}(\theta',S') = \exp\,[-iP_t^{(\sim)}(\theta')] \sum_p \tilde{\Phi}^{(p)}\ \exp\,[ip\omega_t \hat{t}(\theta')], \qquad (B4)$$

where

$$P_t^{(\sim)} = S^{(o)}(\theta' - \theta) - \omega_t S^{(o)}(t' - t) + w_{Di}^{(\sim)}\ , \qquad (B5)$$

so that, using the definition of $w_{Di}^{(\sim)}$,

$$\frac{\partial}{\partial\theta'}\tilde{\phi}(\theta',S') = \{-iS^{(o)} + i\omega_t S^{(o)}\frac{qR_o}{v_{||}(\theta')} - i\frac{qR_o}{v_{||}(\theta')}[\omega_{Di}(\theta') - \omega_{Di}^{(o)}]\}$$

$$\cdot\,\tilde{\phi}(\theta',S') + \sum_p \tilde{\Phi}^{(p)}\frac{ip\omega_t qR_o}{v_{||}(\theta')}\exp\,[ip\omega_t\hat{t}(\theta') - iP_t^{(\sim)}]\ . \qquad (B6)$$

Notice that, from Eqs. (17), (A14), and (A17),

$$\omega_{Di} + S^{(o)}\frac{v_{||}}{qR_o} = \ell\dot{\beta}_{MD} + S\frac{v_{||}}{qR_o} \equiv \omega_{Di(1)} + S\frac{v_{||}}{qR_o}\ . \qquad (B7)$$

Using this result, Eq. (B6) can be rearranged, for $\theta' = \theta$, as

$$[\frac{\partial}{\partial\theta} + iS + i\frac{qR_o}{v_{||}(\theta)}\omega_{Di(1)}(\theta)]\tilde{\phi}(\theta,S) = \frac{iqR_o}{v_{||}(\theta)}\sum_p \tilde{\Phi}^{(p)}\exp\,[ip\omega_t\hat{t}(\theta)]$$

$$\cdot\,\{\omega_{Di}^{(o)} + [p + S^{(o)}]\omega_t\}\ . \qquad (B8)$$

Then obviously

$$\left(\frac{\partial}{\partial\theta} + iS + i\frac{qR_o}{v_{||}}\,\omega_{Di(1)}\right)^2 \tilde{\phi}(\theta,S) = \left(\frac{iqR_o}{v_{||}}\right)^2 \sum_p \tilde{\phi}^{(p)} \exp(ip\omega_t\hat{t}) \cdot \{\omega_{Di}^{(o)} + [p + S^{(o)}]\omega_t\}^2 \quad . \tag{B9}$$

Analogous formulas can be obtained for trapped particles. Using these results in Eq. (B3) gives

$$\tilde{n}_i = -\frac{en}{T_i}\left(\tilde{\phi}(\theta,S) - \frac{1}{n}\int d^3\underset{\sim}{v}\, f_{Mi}(\omega-\omega_{*i}^T) J_o^2 \left\{\left[\frac{1}{\omega} - i\frac{v_{||}}{qR_o\omega^2}\left(\frac{\partial}{\partial\theta} + iS\right)\right.\right.\right.$$
$$\left. + \frac{\omega_{Di(1)}}{\omega^2} - \frac{v_{||}^2}{q^2R_o^2\omega^3}\left(\frac{\partial}{\partial\theta} + iS + i\frac{qR_o}{v_{||}}\,\omega_{Di(1)}\right)^2\right] \cdot \tilde{\phi}(\theta,S) + \ldots$$
$$\left.\left.\left. - i\pi\sum_p \tilde{\phi}^{(p)} \exp(ip\omega_{b,t}\hat{t})\,\delta\{\omega - \omega_{Di}^{(o)} - [p + S^{(o)}H]\omega_{b,t}\}\right\}\right) . \tag{B10}$$

Notice that the two terms in Eq. (B10) which are odd in $v_{||}$ vanish due to the velocity space integral, so that

$$\tilde{n}_i = -\frac{en}{T_i}\left[\tilde{\phi}(\theta,S) - \frac{1}{n}\int d^3\underset{\sim}{v}\, f_{Mi}(\omega-\omega_{*i}^T) J_o^2 \left(\left[\frac{1}{\omega} + \frac{\omega_{Di(1)}}{\omega^2}\right.\right.\right.$$
$$\left. + \frac{\omega_{Di(1)}^2}{\omega^3} - \frac{v_{||}^2}{q^2R_o^2\omega^3}\left(\frac{\partial}{\partial\theta} + iS\right)^2 + \ldots\right]\tilde{\phi}(\theta,S)$$
$$\left.\left.\left. - i\pi\sum_p \tilde{\phi}^{(p)} \exp(ip\omega_{b,t}\hat{t})\,\delta\{\omega - \omega_{Di}^{(o)} - [p + S^{(o)}H]\omega_{b,t}\}\right)\right] . \tag{B11}$$

In Appendix C it is shown that $\omega_{Di(1)} = \bar{\omega}_{Di}\cos\theta(\hat{v}_\perp^2 + 2\hat{v}_{||}^2)$, where $\bar{\omega}_{Di} \equiv \omega_{*i}(r_n/R_o)$, $r_n \equiv -(d\,\ell n\, n/dr)^{-1}$, $v_i \equiv (2T_i/m_i)^{1/2}$, $\hat{v}_{||} \equiv v_{||}/v_i$, and $\hat{v}_\perp \equiv v_\perp/v_i$. The integral

$$\frac{1}{n}\int d^3\underset{\sim}{v}\, f_{Mi}(1-\omega^T_{*i}/\omega)J_0^2(k_\perp v_\perp/\Omega_i)\left[1+\left(\frac{\bar{\omega}_{Di}\cos\theta}{\omega}\right)(\hat{v}_\perp^2+2\hat{v}_{||}^2)\right.$$

$$\left.+\left(\frac{\bar{\omega}_{Di}\cos\theta}{\omega}\right)^2(\hat{v}_\perp^2+2\hat{v}_{||}^2)^2-\frac{v_{||}^2}{q^2R_0^2\omega^2}\left(\frac{\partial}{\partial\theta}+iS\right)^2\right]$$

$$=\frac{2}{\pi^{1/2}}\int_0^\infty d\hat{v}_\perp\,\hat{v}_\perp\exp(-\hat{v}_\perp^2)\int_{-\infty}^{\infty}d\hat{v}_{||}\exp(-\hat{v}_{||}^2)\left\{1-\frac{\omega_{*i}}{\omega}\left[1+\eta_i\left(\hat{v}_{||}^2\right.\right.\right.$$

$$\left.\left.\left.+\hat{v}_\perp^2-\frac{3}{2}\right)\right]\right\}J_0^2(k_\perp\rho_i\hat{v}_\perp)\left[1+\left(\frac{\bar{\omega}_{Di}\cos\theta}{\omega}\right)(\hat{v}_\perp^2+2\hat{v}_{||}^2)+\left(\frac{\bar{\omega}_{Di}\cos\theta}{\omega}\right)^2\right.$$

$$\left.\times(\hat{v}_\perp^4+4\hat{v}_{||}^2\hat{v}_\perp^2+4\hat{v}_{||}^4)-\frac{\bar{\omega}_{ti}^2}{\omega^2}\left(\frac{\partial}{\partial\theta}+iS\right)^2\hat{v}_{||}^2\right]$$

$$=2\int_0^\infty d\hat{v}_\perp\,\hat{v}_\perp\exp(-\hat{v}_\perp^2)J_0^2(k_\perp\rho_i\hat{v}_\perp)\left(\left\{1-\frac{\omega_{*i}}{\omega}\left[1+\eta_i\left(\hat{v}_\perp^2-\frac{3}{2}\right)\right]\right\}\right.$$

$$\times\left[1+\left(\frac{\bar{\omega}_{Di}\cos\theta}{\omega}\right)(\hat{v}_\perp^2+1)+\left(\frac{\bar{\omega}_{Di}\cos\theta}{\omega}\right)^2(\hat{v}_\perp^4+2\hat{v}_\perp^2+3)\right.$$

$$\left.-\frac{\bar{\omega}_{ti}^2}{2\omega^2}\left(\frac{\partial}{\partial\theta}+iS\right)^2\right]+\left(-\eta_i\frac{\omega_{*i}}{\omega}\right)\left[\frac{1}{2}+\left(\frac{\bar{\omega}_{Di}\cos\theta}{\omega}\right)\left(\frac{1}{2}\hat{v}_\perp^2+\frac{3}{2}\right)\right.$$

$$\left.\left.+\left(\frac{\bar{\omega}_{Di}\cos\theta}{\omega}\right)^2\left(\frac{1}{2}\hat{v}_\perp^4+3\hat{v}_\perp^2+\frac{15}{2}\right)\right]\right)\quad, \tag{B12}$$

can be performed by means of standard procedures. To do the $\hat{v}_\perp$-integration we use the general formula[12]

$$\int_0^\infty dt\ t \exp(-pt^2) J_0^2(at) = \frac{1}{2p} \exp(-a^2/2p) I_0\left(\frac{a^2}{2p}\right) , \tag{B13}$$

where I_ν is the modified Bessel function of the first kind. From Eq. (B13)

$$2 \int_0^\infty d\hat{v}_\perp\ \hat{v}_\perp \exp(-\hat{v}_\perp^2) J_0^2(k_\perp \rho_i \hat{v}_\perp) = I_0(b_i) \exp(-b_i) \tag{B14}$$

where $b_i \equiv (1/2) k_\perp^2 \rho_i^2$. By successive differentiation of Eq. (B13) with respect to p, the other needed formulas can be obtained

$$2 \int_0^\infty d\hat{v}_\perp\ \hat{v}_\perp^3 \exp(-\hat{v}_\perp^2) J_0^2(k_\perp \rho_i \hat{v}_\perp)$$

$$= \exp(-b_i)\{I_0(b_i) + b_i[I_1(b_i) - I_0(b_i)]\} , \tag{B15}$$

$$2 \int_0^\infty d\hat{v}_\perp\ \hat{v}_\perp^5 \exp(-\hat{v}_\perp^2) J_0^2(k_\perp \rho_i \hat{v}_\perp)$$

$$= \exp(-b_i)[I_0(b_i)(2 - 4b_i + 2b_i^2) + I_1(b_i)(3b_i - 2b_i^2)] , \tag{B16}$$

and

$$2\int_0^\infty d\hat{v}_\perp\, \hat{v}_\perp^7 \exp(-\hat{v}_\perp^2) J_0^2(k_\perp \rho_i \hat{v}_\perp)$$

$$= \exp(-b_i)\,[I_0(b_i)(6 - 18b_i + 17b_i^2 - 4b_i^3)$$

$$+ I_1(b_i)(11b_i - 15b_i^2 + 4b_i^3)] \quad . \tag{B17}$$

Using these formulas in Eq. (B12), the nonresonant part of $\tilde{n}_i$ is then given by Eq. (23).

The resonant part of the perturbed ion density may be treated in the same way as that for electrons. In particular

$$\delta(\omega - \omega_{Di}^{(o)} - p\omega_b) = \delta(\omega - \hat{\omega}_{Di}^{(o)} X^2 - p\hat{\omega}_b X)$$

$$= \sum_{j''=1}^{2} \delta(X - X_{j''}) \left| p\hat{\omega}_b + 2\hat{\omega}_{Di}^{(o)} X_{j''} \right|^{-1} \quad , \tag{B18}$$

where the $X_{j''}$ are the two roots of the quadratic equation in X in the argument of the second delta function.

As with the electrons, the trapped-ion resonance term does not contain the explicit S-dependence of the circulating-ion resonance term, and therefore will not contribute to the radial structure of the mode in a significant way, and will be dropped. Also terms of order $S^{(\sim)} \equiv S - S^{(o)}$ and $w_{Di}^{(\sim)}$ will be dropped from the circulating-ion resonance term. These terms are not always small, but, since the ion resonance is not localized in S for $\omega > \langle \omega_t \rangle_i$, this omission is not expected to have a

strong effect on the spatial structure either. As is seen in Section IV, the net effect of the ion-resonance term is quite small for realistic parameters, so that the net effect of this omission is also small. The final expression for the resonant part of $\tilde{n}_i$ is then given by Eq. (25).

APPENDIX C

The magnetic drift frequency

$$\omega_{Dj} \equiv \ell\left(\dot{\beta}_{MD} + \{q(r) - q[r^{(o)}]\}\,\frac{d\theta}{dt}\right)$$

$$\simeq \ell\{\dot{\beta}_{MD} + q'[r - r^{(o)}]\,\frac{d\theta}{dt}\} \quad , \tag{C1}$$

where $q' \equiv dq/dr$ is taken as constant, can be put into a more useful form. Now $\dot{\beta}_{MD} \equiv (d\zeta/dt) - q(r)(d\theta/dt) \simeq -(q/r)(v_{MD})_\theta$, with the $(v_{MD})_\zeta$ term being of higher order in $B_\theta^{(o)}/B_o = \epsilon_o/q$. Thus

$$\dot{\beta}_{MD} \equiv -\frac{q}{r}\,\frac{m_j c}{e_j B^3}\,(v_{||}^2 + \tfrac{1}{2}\,v_\perp^2)\,(\underset{\sim}{B} \times \nabla B)_\theta \quad . \tag{C2}$$

Using $B \simeq B_o/h(\theta) = B_o/[1 + (r/R_o)\cos\theta]$, $\nabla B \simeq [B_o/(h^2 R_o)] \times (-\underset{\sim}{e}_r \cos\theta + \underset{\sim}{e}_\theta \sin\theta)$, and $(\underset{\sim}{B} \times \nabla B)_\theta \simeq -[B_o^2/(R_o h^3)]\cos\theta$ gives

$$\dot{\beta}_{MD} \simeq \frac{q}{\Omega_{oj} R_o r}\,(v_{||}^2 + \tfrac{1}{2}\,v_\perp^2)\cos\theta \quad , \tag{C3}$$

where $\Omega_{oj} \equiv e_j B_o/m_j c$. Using Eq. (5) gives

$$r - r^{(o)} \simeq [v_\zeta - v_\zeta^{(o)}]/\Omega_{oj} \simeq [v_{||} - v_{||}^{(o)}]/\Omega_{\theta j}^{o} \quad . \tag{C4}$$

Noting that $d\theta/dt = v_{||}/(qR_o)$, and that

$$\frac{\ell q v^2}{2\Omega_{oj} R_o r} = X^2 \bar{\omega}_{Dj} \tag{C5}$$

where $X \equiv (\varepsilon/T_j)^{1/2}$ and $\bar{\omega}_{Dj} \equiv (r_n/R_o)\omega_{*j}$, the magnetic drift frequency becomes

$$\omega_{Dj} = \bar{\omega}_{Dj} X^2 \left[\left(1 + \frac{v_{||}^2}{v^2}\right) \cos\theta + \frac{q'r}{q} \frac{2}{\epsilon_o} \frac{v_{||}[v_{||} - v_{||}^{(o)}]}{v^2} \right]$$

$$\equiv \omega_{Dj(1)} + \omega_{Dj(2)} \quad . \tag{C6}$$

The time-average $\omega_{Dj}^{(o)}$ of ω_{Dj} is computed in detail in Ref. 13. The result can be expressed in terms of complete elliptic integrals. However, for $q'r/q \sim 1$, $\omega_{Dj}^{(o)}$ can be approximated by $\omega_{Dj}^{(o)} = \bar{\omega}_{Dj} X^2 G$, where the constant $G \sim 1.0$ to 1.2 for trapped particles and $G \simeq 0$ for circulating particles. This approximation facilitates comparison with the local code,[8] where the same approximation is made.

The coefficient function $\tilde{\Phi}^{(p)}$ of the p-th bounce frequency harmonic for trapped particles may be put into a more useful form for computation. Neglecting $S^{(\sim)}$ and $w_{Dj}^{(\sim)}$, Eq. (A26) becomes

$$\tilde{\Phi}^{(p)} = \frac{1}{\tau_b} \oint dt' \exp\left[iS(\theta' - \theta) - ip\omega_b \hat{t}(\theta)\right] \tilde{\phi}(\theta', S) \quad . \tag{C7}$$

Defining a time t_o' such that $v_{||} > 0$ for $t_o' < t' < t_o' + \tau_b/2$ and $v_{||} < 0$ for $t_o' + \tau_b/2 < t' < t_o' + \tau_b$, and using the decomposition (38), $\tilde{\Phi}^{(p)}$ becomes

$$\tilde{\Phi}(p) = \sum_{j,n} \tilde{\phi}_{j,n} h_n(S) \frac{1}{\tau_b} \int_{t_o}^{t_o+\tau_b/2} dt' \left[\exp(iS\theta') g_j(\theta')\right.$$

$$\left. + (-1)^p \exp(-iS\theta') g_j(-\theta')\right] \exp\left[-ip\omega_b \hat{t}(\theta')\right] \exp(-iS\theta) \quad , \qquad (C8)$$

from the symmetry in θ of a trapped-particle orbit. This may be written as a θ'-integration:

$$\tilde{\Phi}(p) = \sum_{j,n} \tilde{\phi}_{j,n} h_n(S) \frac{\epsilon_o^{1/2}}{4\pi L_b(\Lambda)} \int_{0_o}^{\theta_o} d\theta' \frac{\exp\left[-ip\omega_b \hat{t}(\theta')\right]}{\left[1-\Lambda/h(\theta')\right]^{1/2}}$$

$$\times \left[\exp(iS\theta') g_j(\theta') + (-1)^p \exp(-iS\theta') g_j(-\theta')\right] \exp(-iS\theta) \quad , \qquad (C9)$$

where

$$L_b(\Lambda) \equiv \frac{\epsilon_o^{1/2}}{2\pi} \int_{-\theta_o(\Lambda)}^{\theta_o(\Lambda)} d\theta \left[1 - \Lambda/h(\theta)\right]^{-1/2} \quad . \qquad (C10)$$

Similarly, for circulating particles,

$$\tilde{\Phi}(p) = \sum_{j,n} \tilde{\phi}_{j,n} h_n(S) \frac{\epsilon_o^{1/2}}{2\pi L_t(\Lambda)} \int_{-\pi}^{\pi} d\theta' \frac{\exp\left[-i(p+S)\omega_t \hat{t}(\theta')\right]}{\left[1 - \Lambda/h(\theta')\right]^{1/2}}$$

$$\times \exp\left[iS(\theta'-\theta)\right] g_j(\theta') \exp\left[i\omega_t S\hat{t}(\theta)\right] \quad , \qquad (C11)$$

where

$$L_t(\Lambda) \equiv \frac{\epsilon_o^{1/2}}{2\pi} \int_{-\pi}^{\pi} d\theta \left[1-\Lambda/h(\theta)\right]^{-1/2} \quad . \qquad (C12)$$

Using these forms in Eq. (33), the trapped-electron time-average term gives, using the resultant symmetry in θ and θ' from the explicit form of $g_j(\theta)$,

$$K^{l}_{jj',nn'} = -2\pi^{-3/2} \int_0^\infty dX\, X^2 \exp(-X^2)\, \frac{\omega-\omega_{*e}[1+\eta_e(X^2-3/2)]}{\omega + i(\nu_e/\epsilon_o)X^{-3} - \hat{\omega}^{(o)}_{De} X^2}$$

$$\times \int_{-\infty\cdot\sigma^{-1/2}}^{\infty\cdot\sigma^{-1/2}} dS\, h_n(S) h_{n'}(S) \int_0^\pi d\theta \cos[(j'+S)\theta]$$

$$\times \int_{1-\epsilon_o}^{h(\theta)} d\Lambda\, \frac{1}{h(\theta)[1-\Lambda/h(\theta)]^{1/2}}\, \frac{\epsilon_o^{1/2}}{\pi L_b(\Lambda)}$$

$$\times \int_0^{\theta_o(\Lambda)} d\theta'\, \frac{\cos[(j+S)\theta']}{[1-\Lambda/h(\theta')]^{1/2}} \quad . \tag{C13}$$

Similarly the circulating electron resonance (35) gives, setting $\hat{\omega}^{(o)}_{De} = 0$,

$$K^3_{jj',nn'} = \frac{i}{\pi^{1/2}} \int_{-\infty\cdot\sigma^{-1/2}}^{\infty\cdot\sigma^{-1/2}} dS\ h_{n'}(S) h_n(S) \int_0^{1-\epsilon_o} d\Lambda$$

$$\times \int_0^{\pi} d\theta\ \frac{1}{h(\theta)[1-\Lambda/h(\theta)]} \sum_{p=-\infty}^{\infty} \cos\left[(j'+S)\theta - (p+S)\omega_t \hat{t}(\theta)\right]$$

$$\times \sum_{\sigma_{||}=\pm 1} \sum_{j''=1}^{4} H(X^2_{j''}) X^2_{j''} \exp(-X^2_{j''})$$

$$\times \frac{\omega-\omega_{*e}[1+\eta_e(X^2_{j''}-3/2)]}{|(p+S)\hat{\omega}_t(\Lambda)+3i(\nu_e/\epsilon_o)X^{-4}_{j''}|} \frac{\epsilon_o^{1/2}}{\pi L_t(\Lambda)}$$

$$\times \int_0^{\pi} d\theta'\ [1-\Lambda/h(\theta')]^{-1/2} \cos\left[(j+S)\theta' - (p+S)\omega_t \hat{t}(\theta')\right] . \quad (C14)$$

Likewise the ion-resonance term (34) gives

$$K^2_{jj',nn'} = \frac{2i}{\pi^{1/2}} \int_{-\infty \cdot \sigma^{-1/2}}^{\infty \cdot \sigma^{-1/2}} dS\ h_n'(S) h_n(S) \int_0^{1-\epsilon_o} d\Lambda$$

$$\times \int_0^{\pi} d\theta\ \frac{1}{h(\theta)[1-\Lambda/h(\theta)]} \sum_{p=-\infty}^{\infty} \cos\left[(j'+S)\theta-(p+S)\omega_t \hat{t}(\theta)\right] H(X_1^2)$$

$$\times X_1^2 \exp(-X_1^2)\ \frac{\omega-\omega_{*e}[1+\eta_e(X_1^2-3/2)]}{|(p+S)\hat{\omega}_t(\Lambda)|}\ J_o^2[(2b_{i\theta}\Lambda)^{1/2}X_1]\ \frac{\epsilon_o^{1/2}}{\pi L_t(\Lambda)}$$

$$\times \int_0^{\pi} d\theta'\ [1-\Lambda/h(\theta')]^{-1/2} \cos\left[(j+S)\theta'-(p+S)\omega_t \hat{t}(\theta')\right] \quad . \quad \text{(C15)}$$

REFERENCES

[1]W. M. Tang, P. H. Rutherford, E. A. Frieman, and C. S. Liu, Bull. Am. Phys. Soc. 19, 866 (1974).

[2]P. C. Liewer, W. M. Manheimer, and W. M. Tang, Phys. Fluids 19, 276 (1976).

[3]W. Horton, Jr., D. W. Ross, W. M. Tang, H. L. Berk, E. A. Frieman, R. E. LaQuey, R. V. Lovelace, S. M. Mahajan, M. N. Rosenbluth, and P. H. Rutherford, in Plasma Physics and Controlled Nuclear Fusion Research (International Atomic Energy Agency, Vienna, 1975) Vol. I, p. 541.

[4]W. M. Tang, P. H. Rutherford, H. P. Furth, and J. C. Adam, Phys. Rev. Lett. 35, 660 (1975).

[5]P. J. Catto and K. T. Tsang, ORNL Report TM-5237 (1976).

[6]J. D. Callen, C. O. Beasley, S. K. Fischer, H. R. Hicks, and J. F. Seely, Bull. Am. Phys. Soc. 19, 863 (1974).

[7]W. M. Tang, C. S. Liu, M. N. Rosenbluth, P. J. Catto, and J. D. Callen, Nucl. Fusion 16, 191 (1976).

[8]J. C. Adam, W. M. Tang, and P. H. Rutherford, Phys. Fluids 19, 561 (1976).

[9]C. S. Liu, M. N. Rosenbluth, and W. M. Tang, Phys. Fluids 19, 1040 (1976).

[10]M. Abramowitz and I. A. Stegun, Eds., Handbook of Mathematical Functions (National Bureau of Standards, Applied Mathematics Series, Washington, D. C., 1964), Vol. 55, p. 782.

[11]L. D. Pearlstein and H. L. Berk, Phys. Rev. Lett. 23, 220 (1969).

[12]Y L. Luke, Integrals of Bessel Functions (McGraw-Hill, New York, 1962), p. 314.

[13]B. Coppi and G. Rewoldt, in Advances in Plasma Physics, A. Simon and W. B. Thompson, Eds. (Wiley, New York, 1976), Vol. 6, p. 523.

Table I. Chosen and derived parameters of cases considered.

	Chosen Parameters											Derived Parameters			
Case	ϵ_o	T_e/T_i	q	$q'r/q$	η_i	η_e	r_n/r	G	m_i/m_e	ν_e^*	$b_{i\theta}$	$\nu_e/\epsilon_o\omega_{*e}$	$\bar{\omega}_{ti}/\omega_{*e}$	$\bar{\omega}_{te}/\omega_{*e}$	$\rho_i/\Delta r_s$
(a)	0.12	2.	3.5	1.	1.	1.	0.5	1.0	3672	0.158	0.001	1.8	0.383	32.82	0.0447
(b)	0.12	2.	3.5	1.	1.	1.	0.5	1.0	3672	0.00012	0.001	0.00134	---	---	0.0447
(c)	0.25	1.	2.5	1.	1.	1.	1.	1.2	3672	0.06	0.1	0.814	0.447	27.09	0.447
(d)	0.25	2.	2.5	1.	1.	1.	1.	1.2	3672	0.06	0.025	1.15	0.447	38.31	0.224
(e)	0.12	2.	2.5	1.	1.	1.	1.	1.2	3672	0.06	0.025	0.382	0.215	18.42	0.224
(f)	0.25	2.	2.5	1.	-1.	-1.	1.	1.2	3672	0.06	0.025	1.15	0.447	38.31	0.224

Table II. Results for ω and σ from local code and two-dimensional code. Here ω_r and γ are in units of ω_{*e}.

	Local Code				Two-Dimensional Code			
Case	ω_r	γ	σ_r	σ_i	ω_r	γ	σ_r	σ_i
(a)	0.600	0.181	3.95	13.09	0.726	0.029	4.37	[illegible].35
(b)	0.765	-0.037	-0.55	11.31	0.781	-0.009	1.00	[illegible].54
(c)	0.928	0.143	0.162	1.053	0.915	0.125	0.944	[illegible].23
(d)	0.785	0.171	0.530	2.432	0.831	0.178	1.98	0.501
(e)	0.479	0.296	0.896	1.450	0.567	0.23[illegible]	2.12	0.247
(f)	0.493	-0.010	-0.039	1.946	0.590	0.004	[illegible].77	0.800

Table III. Effects on ω_r and γ of turning on and off terms in Eq. (44) for case (d) paraneters. Here ω_r and γ are in units of ω_{*e}.

ion sound	ω_{Di}	ω_{Di}^2, b_{ir}^2	ion res.	electr. res.	ω_r	γ
0	0	0	0	0	0.918	0.315
≠0	0	0	0	0	0.999	0.247
≠0	≠0	0	0	0	0.412	0.196
≠0	≠0	≠0	0	0	0.818	0.210
≠0	≠0	≠0	≠0	0	0.823	0.203
≠0	≠0	≠0	≠0	≠0	0.831	0.178

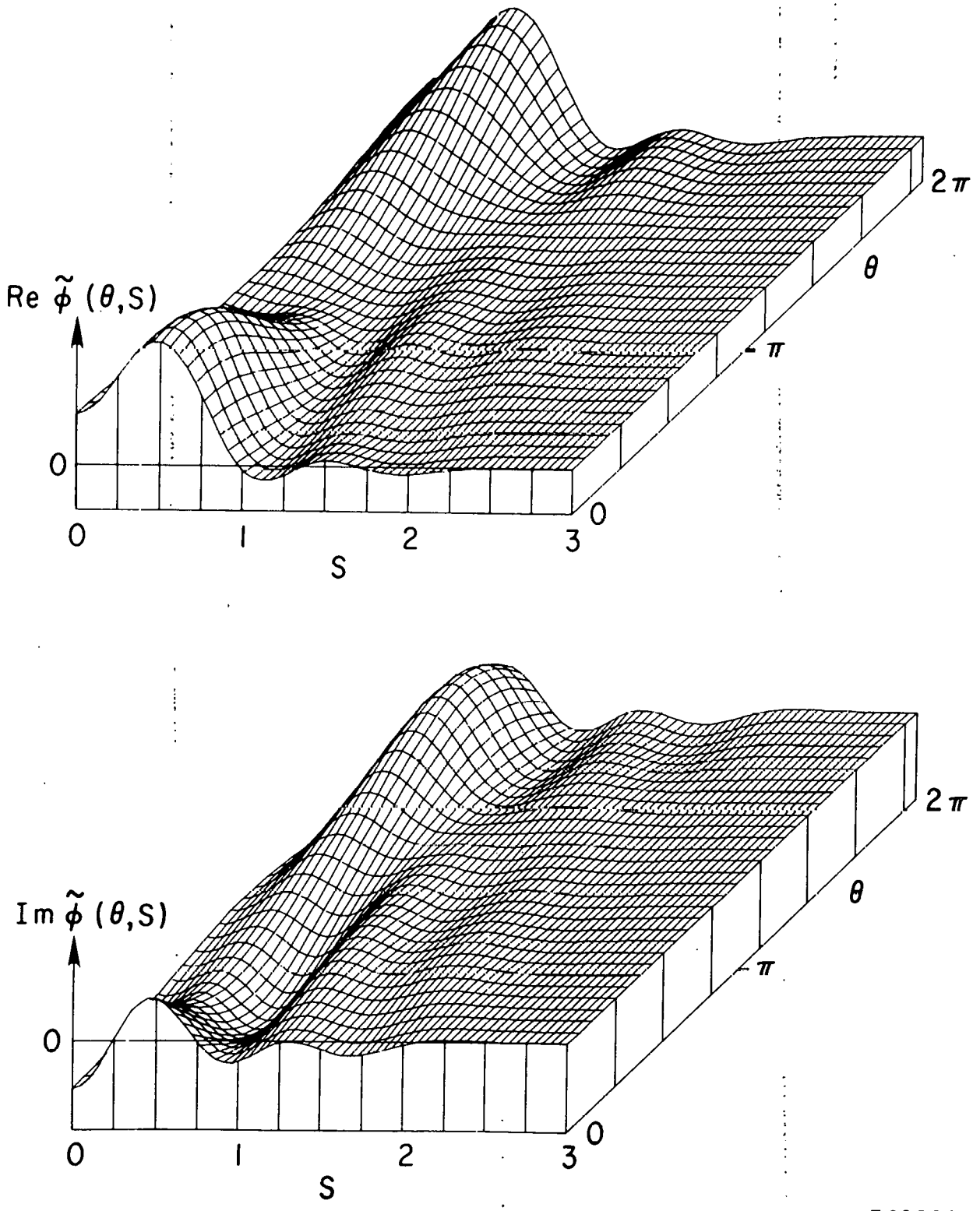

762220

Fig. 1. Real and imaginary parts of the perturbed electrostatic potential eigenfunction $\tilde{\phi}(\theta,S)$ for case (a). Note that the poloidal angle θ is zero at the outside of the torus, and that the radial variable S is $S = (r - r_0)/\Delta r_s$, where r_0 is the radius of the mode-rational surface around which the mode is centered, and Δr_s is the spacing of mode-rational surfaces. Only positive values of S are shown since the eigenfunction is symmetric in $(S\theta)$.

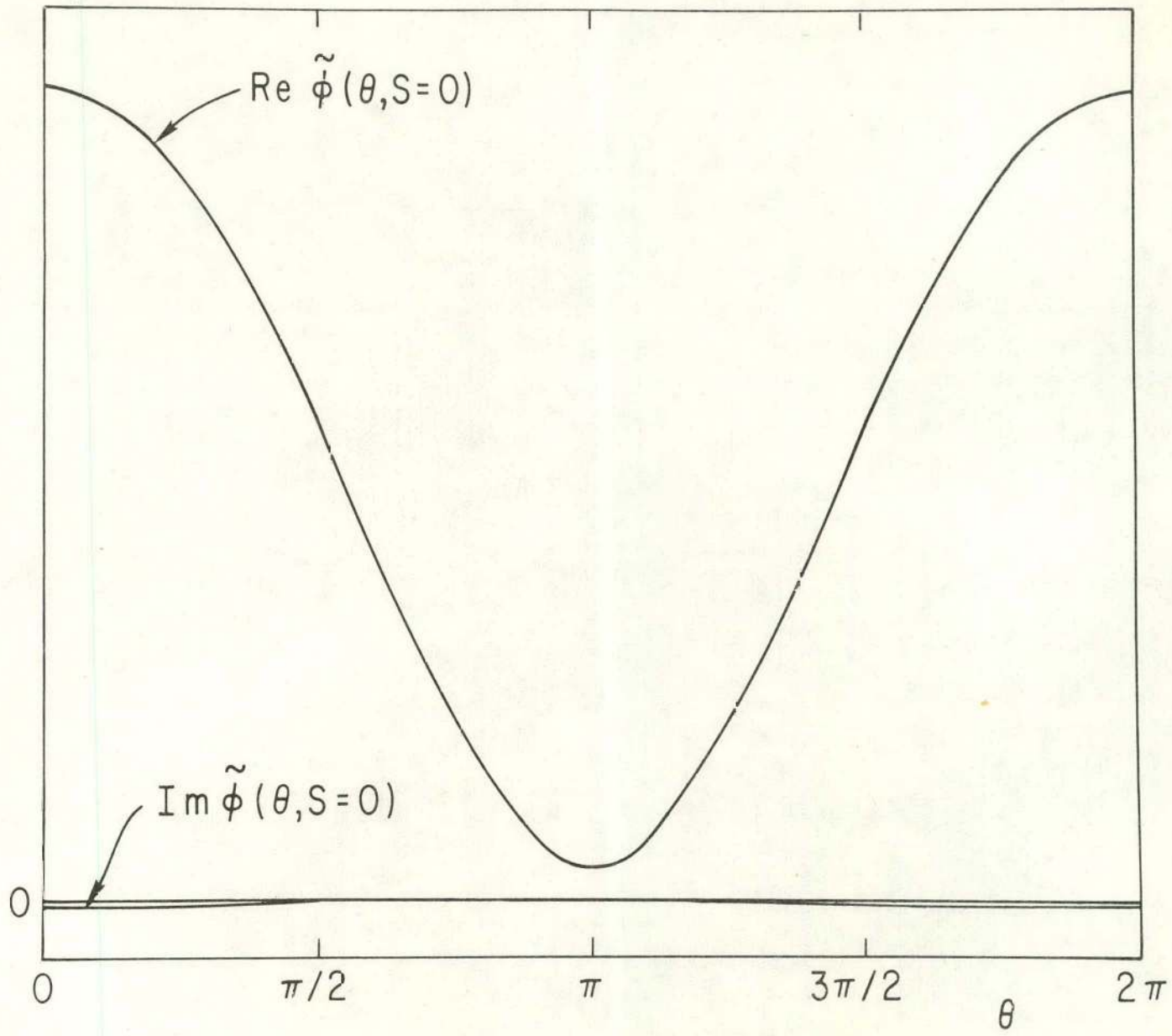

762151

Fig. 2. Real and imaginary parts of $\tilde{\phi}(\theta,S)$ for case (b) at $S = 0$.

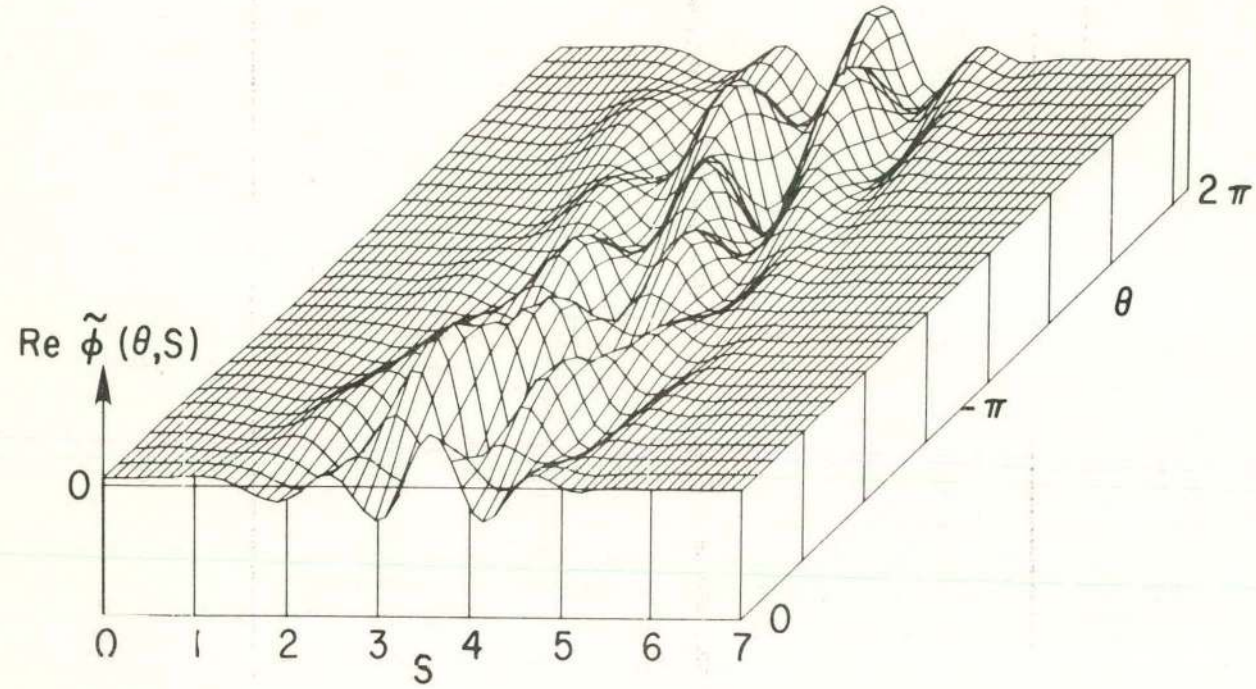

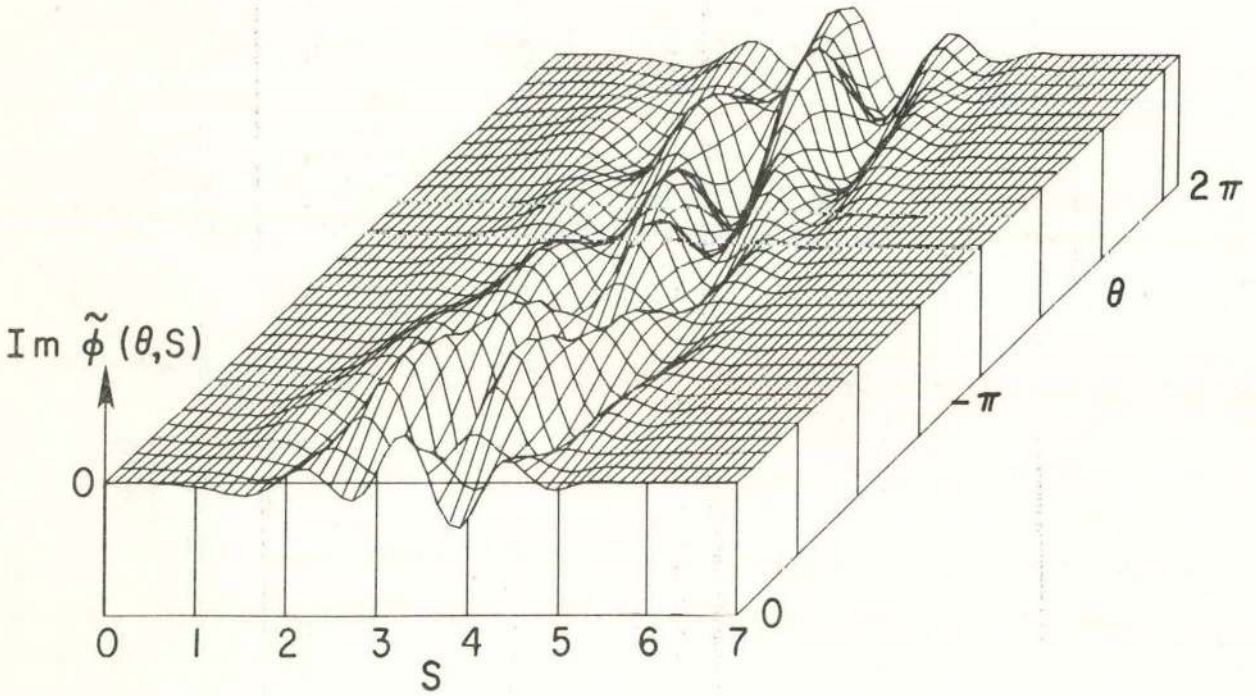

762221

Fig. 3. Real and imaginary parts of $\tilde{\phi}(\theta,S)$ for case (c).

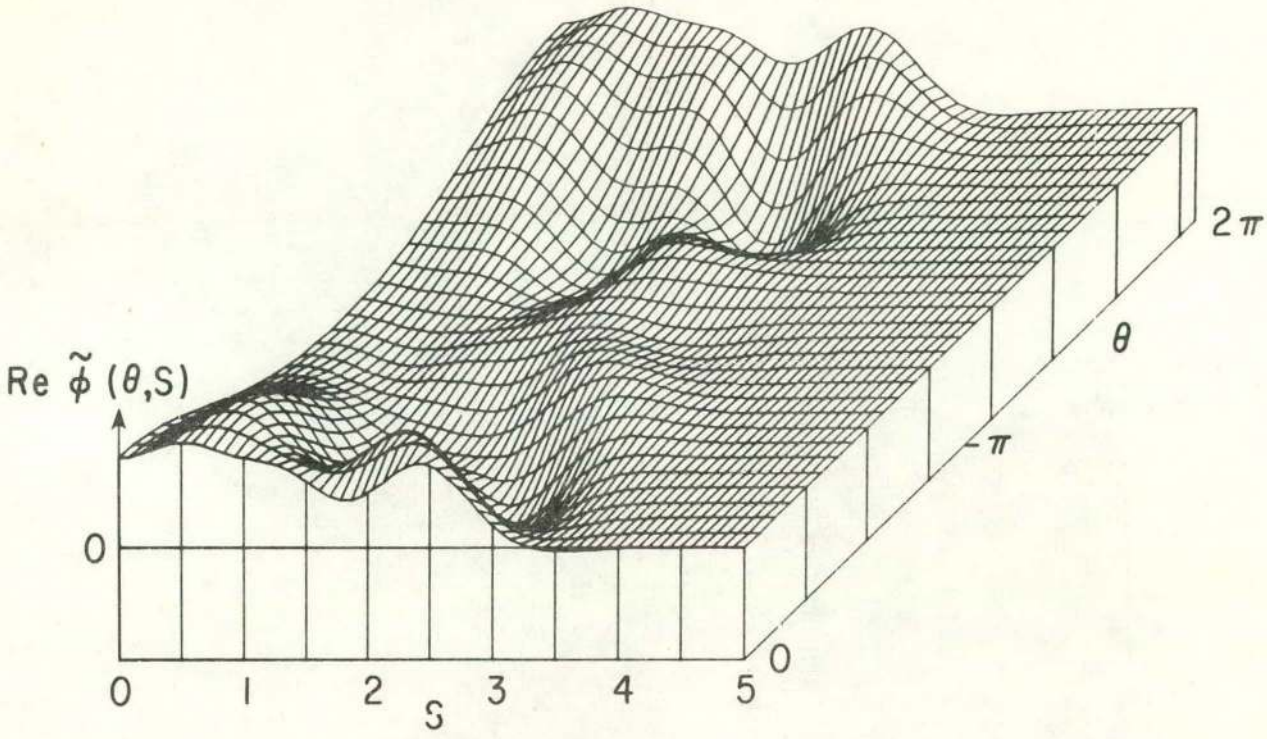

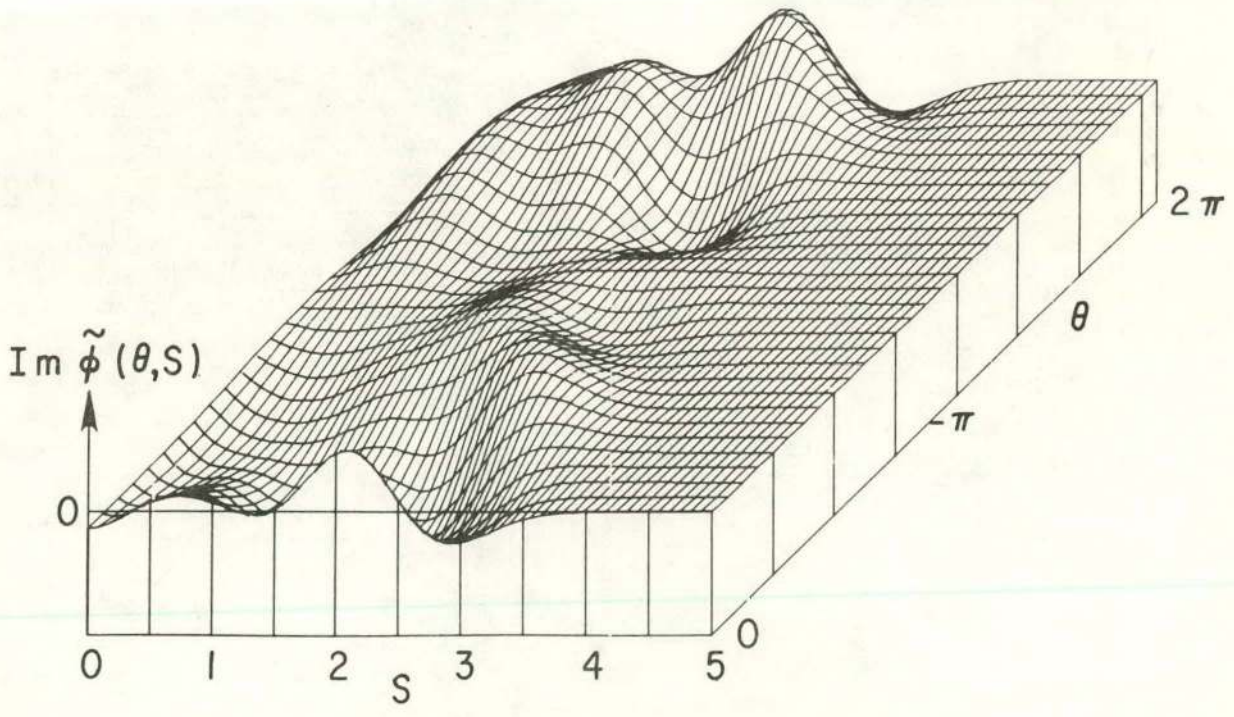

762218

Fig. 4. Real and imaginary parts of $\tilde{\phi}(\theta,S)$ for case (d).

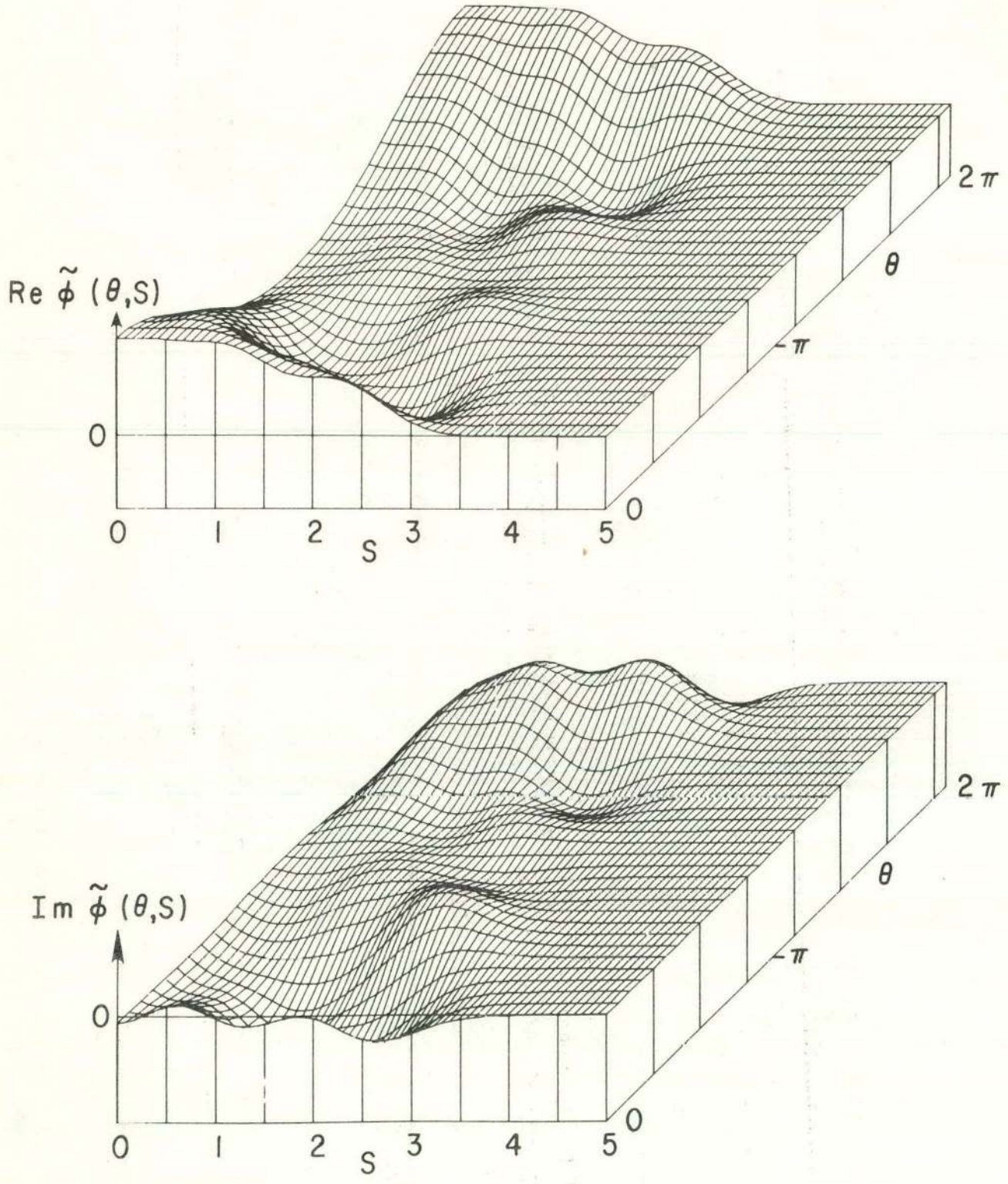

762219

Fig. 5. Real and imaginary parts of $\tilde{\phi}(\theta,S)$ for case (e).

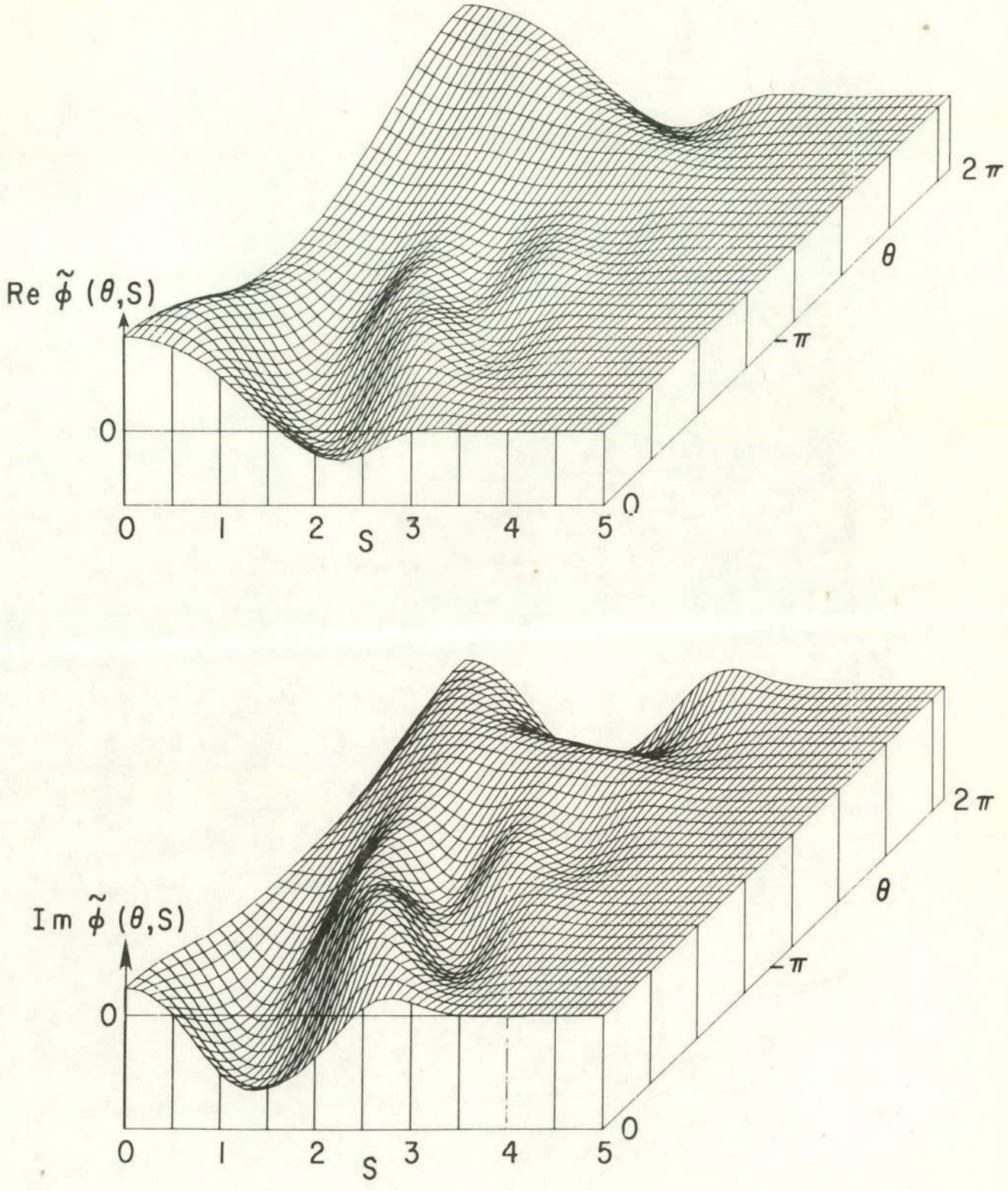

762222

Fig. 6. Real and imaginary parts of $\tilde{\phi}(\theta,S)$ for case (f).